An overview and prospective on Al and Al-ion battery technologies

Journal of Power Sources 481 (2021) 228870

Contents lists available at ScienceDirect

Journal of Power Sources

journal homepage: www.elsevier.com/locate/jpowsour

An overview and prospective on Al and Al-ion battery technologies

Giuseppe Antonio Elia [a,b,*], Kostiantyn V. Kravchyk [c,d,**], Maksym V. Kovalenko [c,d], Joaquín Chacón [e,***], Alex Holland [f], Richard G.A. Wills [f]

[a] Helmholtz Institute Ulm (HIU) Electrochemical Energy Storage, Helmholtzstrasse 11, 89081, Germany
[b] Karlsruhe Institute of Technology (KIT), PO Box, 3640, D-76021 Karlsruhe, Germany
[c] Laboratory of Inorganic Chemistry, Department of Chemistry and Applied Biosciences, ETH Zürich, Vladimir-Prelog-Weg 1, CH-8093 Zürich, Switzerland
[d] Laboratory for Thin Films and Photovoltaics, Empa – Swiss Federal Laboratories for Materials Science and Technology, Überlandstrasse 129, CH-8600 Dübendorf, Switzerland
[e] Albufera Energy Storage, Spain
[f] Energy Technology Research Group, Faculty of Engineering and Physical Sciences, University of Southampton, UK

HIGHLIGHTS

- Recent progress of aluminum-based batteries has been reviewed.
- Overview on aluminum graphite dual-ion batteries (AGDIBs) activity.
- Overview of electrolyte development for aluminum batteries.
- Guidelines and prospective of aluminum battery technology.

ARTICLE INFO

Keywords:
Al batteries
Energy storage
Chloroaluminate melt
Intercalation

ABSTRACT

Aluminum batteries are considered compelling electrochemical energy storage systems because of the natural abundance of aluminum, the high charge storage capacity of aluminum of 2980 mA h g^{-1}/8046 mA h cm^{-3}, and the sufficiently low redox potential of Al^{3+}/Al. Several electrochemical storage technologies based on aluminum have been proposed so far. This review classifies the types of reported Al-batteries into two main groups: aqueous (Al-ion, and Al-air) and non-aqueous (aluminum graphite dual-ion, Al-organic dual-ion, Al-ion, and Al-sulfur). Specific focus is given to Al electrolyte chemistry based on chloroaluminate melts, deep eutectic solvents, polymers, and "chlorine-free" formulations.

1. Introduction

The transition to a sustainable energy economy requires an increase in the share of renewable energy sources (RESs) [1]. However, the large scale implementation of RESs (solar and wind) is hindered by their intermittent nature, geographically uneven energy production, and the lack of suitable storage solutions; currently, there is only 170 GW of installed storage capacity around the world [2]. Renewable electricity production plants, in particular photovoltaic plants, are increasingly needing to control their output to avoid overloading or destabilising the grid [3]. The development of efficient, low-cost, and environmentally-friendly electrochemical storage systems is, therefore, fundamental for the future of the renewable energy economy. Batteries are considered one of the key technologies by the European Union (EU) that can enable the transition to a low-carbon economy through the deployment of batteries in mobility and stationary storage systems. The most mature modern battery technology is the lithium-ion battery (LIB), which is considered the most suitable battery for electromobility because of the high energy density of LIBs. However, long-term, large-scale application of LIBs appears to be problematic due to the natural scarcity and limited production capacity of key materials containing Co and Ni [4]. These factors have motivated the exploration of

* Corresponding author. Helmholtz Institute Ulm (HIU) Electrochemical Energy Storage, Helmholtzstrasse 11, 89081, Germany.
** Corresponding author. Laboratory of Inorganic Chemistry, Department of Chemistry and Applied Biosciences, ETH Zürich, Vladimir-Prelog-Weg 1, CH-8093 Zürich, Switzerland.
*** Corresponding author.
E-mail addresses: giuseppe.elia@kit.edu (G.A. Elia), kravchyk@inorg.chem.ethz.ch (K.V. Kravchyk), joaquin.chacon@albufera-energystorage.com (J. Chacón).

https://doi.org/10.1016/j.jpowsour.2020.228870
Received 1 July 2020; Received in revised form 18 August 2020; Accepted 30 August 2020
Available online 15 September 2020

alternative battery chemistries and concepts, *e.g.*, batteries based on Na [5], K [6], Ca [7], Mg [8] and Al [9,10] ions, which are abundant and non-critical elements [11,12]. Aluminum is attractive because it is lightweight, low cost, and abundant (the most abundant metal in the Earth's crust [9]). An Al metal anode possesses the highest volumetric capacity, 8.04 Ah cm^{-3} (four times higher than Li), which is one order of magnitude higher capacity than the graphite anodes used in conventional LIBs (0.84 Ah cm^{-3}). Furthermore, the gravimetric capacity of 2.98 Ah g^{-1} is also very compelling. In the past five years, research on Al-based electrochemical storage devices has intensified after the publication of Dai and co-workers in 2015 [13]. Here, we survey the present state of research on aluminum-based electrochemical energy storage devices, classifying them into two main sections - aqueous and non-aqueous systems. The aqueous section is divided into two subsections devoted to Al-ion and Al-air batteries. The second part of the review is focused on secondary Al systems employing non-aqueous electrolytes and is divided into two subsections focusing on the electrolytes and cathode materials.

2. Aqueous systems

The use of water-based electrolytes for the realization of aqueous rechargeable batteries ensures an intrinsically safer system, in comparison with non-aqueous batteries. Additionally, the use of water-based electrolytes is expected to have a positive impact on battery cost. Moreover, water-based electrolytes have ionic conductivities approximately two orders magnitude higher than non-aqueous electrolytes, beneficial for the development of high-power systems [14]. However, the narrow electrochemical stability window of aqueous electrolytes (1.23 V), beyond which H_2O decomposes into H_2 and O_2, limits the choice of electrode materials and hence the cell energy density [14]. Nonetheless, aqueous systems can be useful for stationary energy storage, hybridized (multi-device) systems, or e-textiles where reduced energy density is not a prohibitive limitation *per se*.

Additionally, in functional batteries, the operational window can be extended up to 2.0 V by employing electrode materials or electrolyte compositions that inhibit water electrolysis. Overall, aqueous rechargeable batteries are of interest as high power, safe, non-toxic, and potentially low-cost energy storage systems. Aqueous aluminum-ion (Al-ion) batteries [15] are a recent addition to the more widely investigated aqueous metal-ion chemistries which function through the reversible intercalation of cations into host electrodes [16–19]. The interest in Al-systems, which has mostly been driven by lower expected costs and reduced environmental impact over current Li-ion chemistries [20], has pushed new research in the electrochemical storage field. Alternative chemistries could be important for applications where energy density is not prioritized, e.g., where high power, low cost, and safety are needed, and the high unit cost and potential supply risks of lithium are a concern [4,20–22]. The cost of ionic salts used in conventional organic-based electrolytes for supercapacitors ranges between $50-$100/kg, while the solvents acetonitrile and propylene carbonate cost approximately $5-$10/L [23]. For comparison, 5 kg of $AlCl_3{\cdot}6H_2O$ from Alfa Aesar currently costs ≈ $31/kg (May 2020), which is considerably more expensive if the salt were bought in wholesale quantities. However, only a limited number of electrodes have been shown to have a reversible electrochemical capacity in aqueous aluminum-based electrolytes. The high charge density of the Al^{3+} ion, hindering ionic diffusion in host materials, is the main factor responsible for the limited number of available electrode compounds. The use of an aqueous electrolyte can help in shielding the high charge density of metal cations through complexation of the cation with water [24]. In aqueous solutions, Al^{3+} ions form a six coordinated complex (reaction 1). The shielding of the water molecules can have a relevant role in the intercalation mechanism of the Al^{3+} ions. A similar phenomenon has previously been described for Li-ion electrodes [25–27].

$$Al(H_2O)_6^{3+} \rightleftharpoons Al(OH)(H_2O)_5^{2+} + H^+ \quad (1)$$

Regardless, the difficulty of finding suitable electrode material candidates is evident by looking at the limited number of compounds in Table 1, where TiO_2 is the only negative electrode candidate, and V_2O_5 or CuHCF are the only positive electrode materials. Additionally, it should be mentioned that all of the electrochemical characterization reported for aqueous systems has involved three-electrode configurations that use platinum or activated carbon as the counter electrode with an excess of electrolyte. Exceptions to this are the concentrated water-based electrolytes, which are discussed in detail in the last section [28–30]. In the following section, we describe the electrochemical properties of the compounds employed as electrode materials for aqueous Al-ion batteries.

2.1. Electrode materials for aqueous Al-rocking chair batteries

2.1.1. TiO_2

TiO_2 has been widely explored as an active material for Li-ion [31] and Na-ion [32] batteries as well as supercapacitors, using both organic and aqueous electrolytes [33–35]. One of the first attempts of using TiO_2 in aqueous Al-batteries was reported by S. Liu et al., in 2012 [36]. The group prepared TiO_2 nanotubes through the anodization of Ti foil in an NH_4F/water/ethylene glycol electrolyte at 60 V for 30 min at room temperature using a graphite counter electrode. The reported cyclic voltammetry CV of the TiO_2 nanotube electrodes in 1 mol dm^{-3} $AlCl_3$ produced clear reversible redox peaks. The CV tests, performed at various scan rates between 20 mV s^{-1} to 100 mV s^{-1}, revealed there was a shift of the cathodic peaks from approximately −1 V vs. the normal hydrogen electrode (NHE) at 20 mV s^{-1} to −1.1 V vs. NHE at 100 mV s^{-1}, and an anodic shift from approximately −0.6 V to −0.52 V vs. NHE. The linearity of the peak currents with respect to the square root of the scan rate suggested a diffusion-limited process, which was attributed to solid-state diffusion of Al^{3+} through the electrode. The prepared electrode had a capacity of 75 mA h g^{-1} at 4 mA cm^{-2}, with a coulombic efficiency approaching 90% (Fig. 1). Ex-situ X-ray photoelectron spectroscopy (XPS) spectra of cycled electrodes revealed there was a variation of the titanium oxidation state as a function of the state of charge, suggesting the involvement of the Ti in the redox process.

The electrochemical activity of TiO_2 in aqueous aluminum electrolytes was confirmed by Y. Liu et al. [37]. The group prepared TiO_2 electrodes using an anodization process similar to Refs. [36]. Their TiO_2 electrodes were investigated by CV and electrochemical impedance spectroscopy (EIS). The CV tests revealed there was a linear relationship between the peak current density and the square root of the scan rate, in agreement with S. Liu et al. [36]. The study showed that the peak current increased for increased additions of NaCl to the $Al_2(SO_4)_3$ electrolyte. Moreover, EIS measurements revealed there was a reduction in the charge transfer resistance for increased additions of NaCl to the electrolyte. However, a clear explanation of how Cl^- assisted the insertion of Al^{3+} was not given. Aurbach et al. demonstrated a similar phenomenon for Mg-batteries [38]. Nonetheless, the possible role that Na^+ ions had in improving the electrochemical behavior should also be considered. Kazazi et al. investigated the properties of TiO_2 nanospheres in aqueous Al-cells [39]. Galvanostatic cycling tests performed in 1 mol dm^{-3} $AlCl_3$ electrolyte revealed a good discharge capacity of 180 mA h g^{-1} at a 0.15 C rate and a capacity of 105 mA h g^{-1} at 6 C (10-min charge). However, the system showed a 6% capacity fade over 30 cycles during the test,

Table 1
Summary of known aqueous Al-ion electrodes reported in the literature. Coulombic efficiencies estimated from charge/discharge voltage profiles.

Electrode and Electrolyte	Specific Capacity	Cyclability	Coulombic Efficiency	Voltage range/profile	Reference
***Half-cell** – graphene-TiO_2. $AlCl_3$*	*25*-10 mA h g^{-1}	*≃ 50% fade over 125 cycles*	*≃ 50%*	*-0.85 V – -0.3 V vs NHE*	[40]
***Half-cell** – TiO_2 nano-spheres. 1 M $AlCl_3$*	180 mA h g^{-1} @ 50 mA g^{-1} 105 mA h g^{-1} @ 2010 mA g^{-1}	*≃ 6% fade over 30 cycles*	*≃ 90%* @ 2000 mA g^{-1}.	*-1 V – -0.1 V vs NHE. Discharge plateau @ -0.75 V – -0.7 V vs NHE.*	[39]
***Half-cell** – TiO_2 nano-wire array film. Various inc. 0.5 M $Al_2(SO_4)_3$*	75 mA h g^{-1} @ 4 mA cm^{-2}	-	*≃ 85%*	*-0.9 – -0.7 V/Discharge plateau just below 1 V*	[37]
***Half-cell.** TiO_2 nano-tube array film. 1 M $AlCl_3$*	75 mA h g^{-1} @ 4 mA cm^{-2}	-	*≃ 90%*	*-0.95 and -0.16 V vs/Discharge plateau ≃ -0.76 V vs NHE*	[36]
***Half-cell.** TiO_2. 1 M $AlCl_3$*	15 mA h g^{-1} @ 4 A cm^{-2}	*≃ 5% fade over 1000 cycles @ 4 A g^{-1}*	*≃ 100% @ 4 A g^{-1}*	*-1.0 – 0.2 V vs NHE*	[53]
***Half-cell** – CuHCF. 0.5 M $Al_2(SO_4)_3$*	41 mA h g^{-1} @ 400 mA g^{-1}	*45% fade over 1000 cycles*	*≃ 100%*	*0.44 – 1 V vs NHE. No plateau.*	[49]
***Half-cell** - V_2O_5 aerogel. 1 M $AlCl_3$*	120 mA h g^{-1} @ 60 mA g^{-1} ~15 mA h g^{-1} @ 200 mA g^{-1}	*≃ 40% fade @ 60 mA g^{-1} and ≃ 25% fade @ 200 mA g^{-1} over 13 cycles*	*≃ 85%*	*-0.24 V – 0.49 V vs NHE. Discharge plateau @ -0.49 V.*	[52]

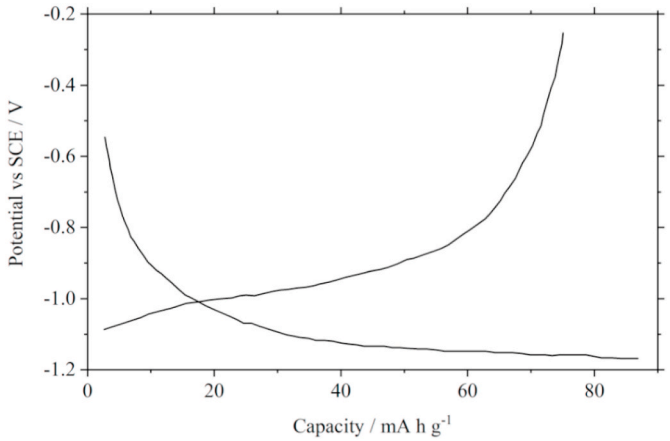

Fig. 1. The charge/discharge curve of a TiO_2 NTA electrode in 1 mol dm^{-3} $AlCl_3$ cycled at a current density of 4 mA cm^{-2}. The graph has been adapted from Ref. [36].

with a coulombic efficiency of approximately 90%. The prepared material was compared with commercial TiO_2 nanopowder (Aeroxide® P25-Sigma Aldrich), which showed that the TiO_2 nanospheres had better performance. Recently Lahan et al. [40] evaluated the use of graphene in the preparation of TiO_2 electrodes, which resulted in TiO_2 nanoparticle electrodes with improved storage capacities of 20 mA h g^{-1} at 6.25 A g^{-1}. However, the system was characterized by a low coulombic efficiency of approximately 50% (as estimated from the graphical data) [40].

Accordingly, to the various reports, the aluminum insertion process can be expressed as (2):

$$TiO_2 + xAl^{3+} + xe^- \rightleftharpoons Al_xTiO_2 \quad (2)$$

However, the potential contributions of protons to the electrochemical reaction needs clarification, similar to the case of Zn [41–44]. Moreover, various reports have shown that aqueous TiO_2 systems have low coulombic efficiency [36,37,39]. We can identify three reasons for the low coulombic efficiency:

- The insertion of Al^{3+} into anatase TiO_2 may lead to a partially irreversible process [36].
- Dissolved O_2 may interfere with the electrochemical process (Ti^{3+} is known to be oxidized by atmospheric O_2) [45].
- H_2 evolution can take place. The side reaction starts at approximately −0.2 V vs. SHE for pH 3 solutions, although H_2 evolution may be hindered by kinetics and the strong solvation of the Al^{3+} ions. Indeed, CVs show that H_2 evolution occurs at reduced potentials, lower than the peaks attributed to Al^{3+} insertion.

Any combination of the above would naturally lead to lower coulombic efficiency. The first point highlights that the reaction process needs to be investigated further, and the role of the intercalation mechanism must be clarified [37,46]. The second point can be mitigated by degassing the electrolyte before use. Aqueous Li-ion batteries have shown marked improvements when operated in O_2-free electrolytes [47].

2.1.2. *Prussian blue*

Hexacyanoferrates and Prussian blue analogs are interesting electrode materials due to their open framework structure that can host a variety of guest ions (Li^+, Na^+, Mg^{2+}, etc.) [48]. Liu et al. [49] evaluated the use of $KCu_2[Fe(CN)_6]$. xH_2O (CuHCF) in aqueous Al-ion systems using a 0.5 mol dm^{-3} $Al_2(SO_4)_3$ electrolyte. The CVs showed broad reversible peaks with multiple shoulders demonstrating the redox activity of the compound. Galvanostatic cycling also showed sloping charge/discharge curves as opposed to the desired plateau, with a 45% capacity fade over 1000 cycles. The cause of this capacity fade was not discussed.

2.1.3. *V_2O_5*

Vanadium oxide-based materials are promising electrode materials [50] that have large tunnels or interlayer space for cation intercalation [51]. González et al. evaluated the use of V_2O_5 xerogels in aqueous Al-cells employing a 1 mol dm^{-3} $AlCl_3$ electrolyte [52]. The CV tests performed at 10 mV s^{-1} revealed reversible redox peaks at 0.39 V and 0.64 V vs. NHE. The galvanostatic cycling tests at 60 mA g^{-1} revealed an initial capacity of approximately 120 mA h g^{-1}, which reduced to 75 mA h g^{-1} after 13 cycles. Cycling at 200 mA g^{-1} produced a more stable response; however, the measured capacity was only ca. 20 mA h g^{-1} and reduced to less than 10 mA h g^{-1} after 13 cycles.

2.2. *Al metal*

Lynden Archer recently proposed the possibility of using Al stripping/deposition in a water-based electrolyte creating “artificial interphase” by treating the Al metal (T-Al) with conventional chloroaluminate melts [28]. Treating the Al metal with conventional chloroaluminate led to partial removal of the Al_2O_3 passivation layer

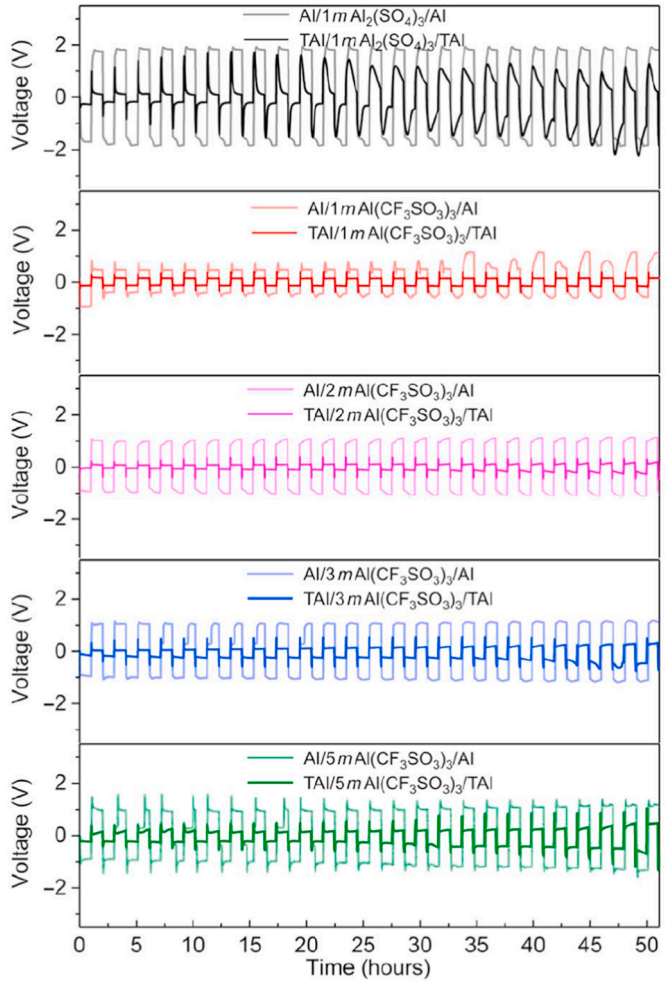

Fig. 2. Symmetric Al-battery tests using Al and T-Al electrodes coupled with different electrolytes. The current density was 0.2 mA cm^{-2} with a time limitation of 1 h for the charge/discharge process [28].

and the formation of a layer rich in Al, Cl, and N at the electrode's surface [28]. The group evaluated the use of $Al(CF_3SO_3)_3$ in H_2O at various concentrations in symmetrical T-Al/H_2O–$Al(CF_3SO_3)_3$/T-Al cells by performing galvanostatic cycling tests at a current of 0.2 mA cm^{-2} (Fig. 2). The authors associated the charge/discharge voltage profile of symmetrical T-Al/T-Al cells with the Al stripping deposition process. The flat voltage profile upon time suggests a stripping deposition process where Al ions are released from the counter electrode (T-Al), following their electrodeposition at the working electrode (T-Al), when negative current is applied, and vice versa when a positive current is applied. The authors indicated the 1 and 2 m $Al(CF_3SO_3)_3$ electrolyte solutions as the best composition, characterized by an overvoltage of approximately 0.2 V. The same approach has been used by other groups that obtained similar voltage profiles associated with the Al stripping/deposition process [29,30]. The possibility of a reversible Al stripping/deposition process in such a condition is extremely promising. However, further investigations are required to clarify the reaction mechanism.

2.2.1. MnO_2

The use of MnO_2 as an electroactive material for Al-batteries was proposed and tested by Lynden Archer [28] in Al-battery cells using a 3 m $Al(CF_3SO_3)_3$ electrolyte and an Al metal anode pretreated with a 1:1.3 EMIMCl:$AlCl_3$ electrolyte. The pre-treatment of Al metal (T-Al) improves the stripping deposition process at the negative electrode (see the previous section for details). The proposed cell configuration delivered approximately 350 mA h g^{-1} of charge in the initial cycles with an average discharge voltage of approximately 1.4 V. However, the delivered capacity rapidly faded to around 200 mA h g^{-1} after the first 10 cycles. The reaction mechanism was investigated by ex-situ XRD, SEM and TEM, all of which indicated a reversible surface process with the formation of water-soluble products, suggesting that the Al^{3+} ions did not intercalate into the MnO_2. Similar results have been reported recently by He et al. [54] for a system using a Birnessite MnO_2 cathode [29] and a treated Al-metal anode (T-Al). The report demonstrated the beneficial effects of using $MnSO_4$ as an additive (0.5 m) in the 2 m Al $(CF_3SO_3)_3$ electrolyte, with a 40% improvement in the initial discharge capacity ($MnSO_4$-free electrolyte 350 mA h g^{-1}, electrolyte with added Mn 550 mA h g^{-1}). Investigation of the reaction mechanism indicated that conversion of the initial MnO_2 phase occurred in the first discharge, and a new Mn compound was formed during the first charge process, which then served as the reversible cathode active material in the following cycles. Moreover, their investigations suggested that Mn^{2+} was also involved in the electrochemical reaction. A similar cell configuration has also been reported by Wu et al. [30], using Mn_3O_4 as the electrode material. They performed electrochemical oxidation of the Mn_3O_4 in a 5 M $Al(CF_3SO_3)_3$–H_2O electrolyte, the results of which suggested a spinel-to-layered structural evolution occurred for the Mn_3O_4, along with the formation of an $Al_xMnO_2{\cdot}nH_2O$ phase, which was determined to be the electroactive material. The results of all the studies on the T-Al/MnO_2 system indicate that this technology is still in the preliminary stage and further studies are needed to clarify the overall electrochemical mechanism. The metrics (gravimetric capacity and working voltage) do however suggest that this cell configuration is promising.

3. Primary Al-air battery

Aluminum has continuously drawn considerable attention as a potential battery anode because of its high theoretical voltage and capacity while being an element of small size. Furthermore, the ability of aluminum ions to exchange up to three electrons in every oxidation-reduction reaction has been a key motivator for the use of aluminum-based systems in the electrochemical and energy industries. However, these exceptional properties are not achievable in practical batteries because of the inability to operate aluminum and air electrodes at their thermodynamic potentials. Additionally, a significant quantity of water is consumed during the discharge reaction. Even with these limitations, the energy density values are higher than those of the majority of battery systems [55].

Several reviews have been carried out since the first studies on this technology [56]. The most recent research has mainly been focused on improving the catalytic performance of the air electrode by utilizing new advanced catalysts based on metal oxides. However, there have not been demonstrations of better practical metrics [56]. The implementation of the Zn-air battery for some niche applications has left little space in the market for the development of commercial aluminum-air batteries.

The inherent hydrogen generation at the aluminum anode in aqueous electrolytes is so substantial that aluminum-air batteries are usually designed as reserve systems, with the electrolyte being added just before use, or as "mechanically" rechargeable batteries where the aluminum anode is replaced after each discharge cycle.

The discharge reactions for the aluminum-air cell are:

$$\text{Anode: Al} \longrightarrow Al^{+3} + 3\ e^- \quad (3)$$

$$\text{Cathode: } O_2 + 2H_2O + 4\ e^- \longrightarrow 4\ OH^- \quad (4)$$

$$\text{Overall: } 4\ Al + 3\ O_2 + 6H_2O \longrightarrow 4\ Al(OH)_3 \quad (5)$$

With the parasitic hydrogen-generating reaction:

$$Al + 3H_2O \longrightarrow Al(OH)_3 + 3/2H_2 \quad (6)$$

Aluminum can be discharged in neutral salt solutions as well as in alkaline solutions. The use of neutral electrolytes [57] is attractive because of the relatively low open-circuit corrosion rates and the reduced hazard of neutral solutions. Saline systems are appropriate for low power applications, with measured specific energy values up to 800 Wh/kg.

Alkaline systems have an advantage over neutral salt systems because alkaline electrolytes have higher conductivity and a higher solubility for the aluminum hydroxide reaction product. Accordingly, alkaline aluminum-air batteries are a suitable candidate for high power applications such as standby batteries, as propulsion power sources for autonomous underwater vehicles, and has been proposed for electric vehicle propulsion [58]. The specific energy of these batteries can be as high as 400 Wh/kg, which enables their use as reserve energy sources in remote areas.

Aluminum-air batteries with high energy and power densities were described in the early 1960s. However, practical commercialization never began because this system presents some critical technological limitations. These market limiting features are related to the high open-circuit corrosion rate of aluminum alloys in alkaline electrolytes, the unavailability of thin, large dimension air cathodes, and the difficulty of managing the cell reaction products. However, significant advances have been made in improving these characteristics since aluminum-air batteries were first introduced [59]. Recently, Hopkins et al. [60] proposed displacing the aqueous electrolyte with oil to suppress corrosion. Although this system has negligible self-corrosion (<0.02% a month), the additional equipment required for maintaining a continuous flow of electrolyte and the storage and handling of the oil would add a significant amount of weight to the system.

One of the intrinsic drawbacks of the Al-air system is non-rechargeability. However, this limitation can be overcome by utilizing Al-metal as an energy carrier in a circular energy economy.

Hydrogen is a well-known energy carrier that can be utilized in the future in the energy sector for stationary and mobile applications. However, few studies [61] explored the possibilities of employing aluminum metal as an efficient energy carrier. Aluminum is easy to transport and store since it is covered by a passivating oxide film that protects the surface of the metal from corrosion [62] and prevents damage to the material during periods of transport and storage. Aluminum is considered a renewable source of energy as it has a high calorific value, is abundant in the earth's crust [11,63], and the production of aluminum occurs in almost every country [64–66]. For these reasons, aluminum represents a suitable energy carrier from many different points of view.

However, the aluminum production industry consumes a significant amount of electricity, which is considered a barrier to the use of Al-metal in the energy field. However, the growth of renewable electricity sources has created new opportunities for the use of Al-metal as energy storage since production facilities can be installed close to green electricity sources.

The actual efficiency of the aluminum energy cycle is lower than 43%. Nevertheless, this depends on the application. It is well known that 2 kg of alumina, 0.5 kg of coal, and approximately 0.05 kg of cryolite are needed to produce 1 kg of aluminum. Furthermore, the power required for this process is estimated to be between 13 and 20 kWh of electrical energy, which is ca. 100 MJ/kg for the whole process [61].

The electrochemical oxidation of aluminum in aqueous alkaline solutions (Al-air battery) is the most efficient method. Al-air batteries have been proposed as the power source for vehicles, where a mechanical recharge process is carried out by replenishing the metal upon complete consumption by the oxidation process. Phinergy and Alcoa have made significant investments in this direction [58]. The direct electrochemical oxidation reaction provides 4300 Wh/kg (theoretical) of specific energy at approximately 55% electrical efficiency. Technologies based on the chemical oxidation of aluminum reach specific energies of 1040 Wh/kg with 25% electrical efficiency. For stationary storage applications, high-temperature processes, and aluminum reactions in neutral or alkaline water solutions are more appropriate. In this case, the theoretical electrical efficiency can reach 45%, while the specific energy can reach values of 8600 Wh/kg (theoretical) [60]. However, side reactions and hydrogen evolution also severely reduce the practical value of these systems.

4. Non-aqueous Al-batteries

4.1. Non-aqueous electrolytes for Al-batteries

This section is based on a survey of the literature from the past five years (2015–2020) on electrolyte systems for Al-battery applications (Table 2). Fig. 3 shows that chloroaluminate melts are the most widely used electrolyte composition. Imidazolium based electrolytes are the most popular, and only a minor number of reports are dedicated to investigations of alternative chloroaluminate melt compositions. Even though $AlCl_3$-ImidazoliumCl ($AlCl_3$-Im) is considered the state of the art electrolyte for Al-batteries, efforts have been dedicated to finding alternative chloroaluminate systems. Moreover, the use of polymer electrolytes has also been investigated. Finally, some reports have introduced the concept of "Cl-free" electrolytes. This section of the review is divided into four main parts. The first describes chloroaluminate melts, and the following section discussed the corrosivity issues of this system. The following section explores polymer electrolytes, and the final section discusses Cl-free electrolytes.

4.1.1. Chloroaluminate melts

Chloroaluminate melts were the first generation of ionic liquids (ILs) [201]. Their origin can be dated back to 1948 when Hurley and Wier developed a chloroaluminate melt as a bath solution for electroplating aluminum [202]. The scientific community started showing interest in the late 1970s with the studies of Oster Young, and Wilkes [203,204]. Chloroaluminate melts are a mixture with a general formula of MCl-$AlCl_3$, where M^+ can be a monovalent cation like Li^+, Na^+, K^+, or an organic cation like pyrrolidinium or imidazolium [202–205]. The use of an organic cation reduces the melting point to below 100 °C [203,204]. The ionic speciation of the ionic liquid (IL) is basic, neutral, or acidic when the MCl/$AlCl_3$ mole ratio is higher, equal, or lower than one,

Table 2
List of electrolyte composition obtained from a survey of 133 Al-battery papers.

Electrolyte composition	References
$AlCl_3$-ImidazoliumCl	[10,13,67–161]
$AlCl_3$-1-methyl-1-propylpyrrolidinium chloride	[162]
$AlCl_3$-ImidazoliumCl, chain length investigation	[163]
$AlCl_3$-Benzyltriethylammonium chloride	[164]
$AlCl_3$-Triethylamine hydrochloride	[165–168]
$AlCl_3$-Imidazole hydrochloride	[169]
$AlCl_3$-1-trifluoroacetyl piperidine	[170]
$AlCl_3$-EMIMBr	[171–173]
$AlCl_3$-Urea	[86,174–179]
$AlCl_3$-Acetamide	[86,175,180]
$AlCl_3$-Propionamide	[175]
AlC_3-Butyramide	[175]
$AlCl_3$-Caprolactam	[181]
$AlCl_3$-4-ethylpyridine	[182]
$AlCl_3$-Dipropylsulfone-Toluene	[183,184]
$AlCl_3$-Urea-1-ethyl-3-methylimidazoliumCl ternary electrolyte	[185]
$AlCl_3$-Polymer based electrolyte	[186–191]
$AlCl_3$–H_2O	[192]
$Al(CF_3SO_3)_3$-1-butyl-3-methylimidazolium trifluoromethanesulfonate	[193]
$Al(CF_3SO_3)_3$-Diglyme	[194]
$Al(CF_3SO_3)_3$–*N*-methylacetamide-Urea	[195]
$[Al(1\text{-butylimidazole})_6][TFSI]_3$	[196]
$Al(TFSI)_3$-Acetonitrile	[197]
$Al(CF_3SO_3)_3$–H_2O	[28–30, 198–200]

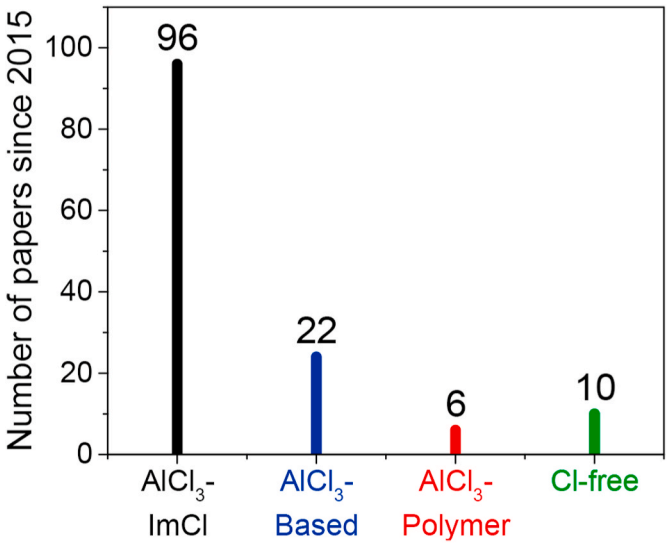

Fig. 3. Number of papers since 2015 dealing with Al-based rechargeable batteries using $AlCl_3$-Imidazolum, $AlCl_3$-based, $AlCl_3$-polymer and Cl-free electrolytes. The survey has been done using the papers listed in Table 2. (last updated on May 1, 2020). The keywords used for the search in the Scopus database were "Aluminum battery".

respectively [206]. The ionic speciation is governed by equilibrium defined in equation (7) [206]:

$$2AlCl_4^- \leftrightarrow Al_2Cl_7^- + Cl^- \quad (7)$$

For basic melts $AlCl_4^-$ and Cl^- coexist, in neutral melts only $AlCl_4^-$ is present, and in acidic melts there is the formation of $Al_2Cl_7^-$. The latter species has been identified as a key compound for the reversible Al stripping/deposition process [206–211]. The drawback of using chloroaluminate melts is their moisture sensitivity since chloroaluminate melts are extremely hygroscopic, labile towards hydrolysis, and highly corrosive [9]. These limitations have pushed the scientific community to find alternative anions in order to obtain air-stable, non-corrosive ILs. An alternative was identified in 1992 by Wilkes and Zaworotko, who introduced the CH_3CO_2, NO_3, and BF_4 anions [212]. However, the interest in chloroaluminate melts never faded completely, mostly due to their ability to electrodeposit Al-metal efficiently [208,210]. Recently, interest in this class of IL has grown again, driven by the need to find alternative electrochemical storage systems based on abundant and low-cost elements such as Al [9,11–13,213]. However, the main drawbacks of chloroaluminate melts remain unresolved. The ability of the chloroaluminate melts to efficiently sustain the Al stripping/deposition process required for electrochemical storage systems relies on two main phenomena. The first is associated with the high corrosivity of the chloroaluminate melts, capable of removing the native Al_2O_3 passivation layer [210]. The second is the presence of $Al_2Cl_7^-$ in the melt [206–211]. These two factors limit the choice of suitable electrolytes for Al-battery applications. Indeed, most of the reports in the past five years have used $AlCl_3$-Im based electrolytes (Fig. 3). A new class of ionic liquids referred to as deep eutectic solvents (DESs), or ionic liquid analogs (ILAs), are generally formed through a mixture of a strongly Lewis acidic metal halide and a Lewis basic ligand and have gained significant attention due to their comparable electrochemical and physical properties at reduced costs and minimal environmental impact [214]. Abood et al. first disclosed a DES derived from a mixture of $AlCl_3$ and an oxygen donor amide ligand (urea or acetamide), in which ions were formed through the heterolytic cleavage of $AlCl_3$ (the Al_2Cl_6 unit) giving $AlCl_4^-$ anions and $[AlCl_2{\cdot}(ligand)_n]^+$ cations, where the latter were suggested to be responsible for reductive aluminum deposition [214]. Since then, numerous different Lewis basic ligands have been shown to form DESs when mixed with $AlCl_3$, which are capable of effective aluminum deposition [215–217]. The application of this class of electrolytes in Al-batteries was introduced in 2017 [174,176] for use in Al/graphite cells employing an $AlCl_3$:urea electrolyte (1.3:1 mole ratio). The two reports demonstrated that the use of a urea-based electrolyte leads to better coulombic efficiencies in Aluminum graphite dual-ion batteries (AGDIBs). Dai's group used Raman and NMR spectroscopy to show the existence of $AlCl_4^-$, $Al_2Cl_7^-$ anions and $[AlCl_2{\cdot}(urea)_n]^+$ cations in the $AlCl_3$/urea electrolyte when an excess of $AlCl_3$ was present [174]. Following their initial work, Dai's group evaluated the properties of

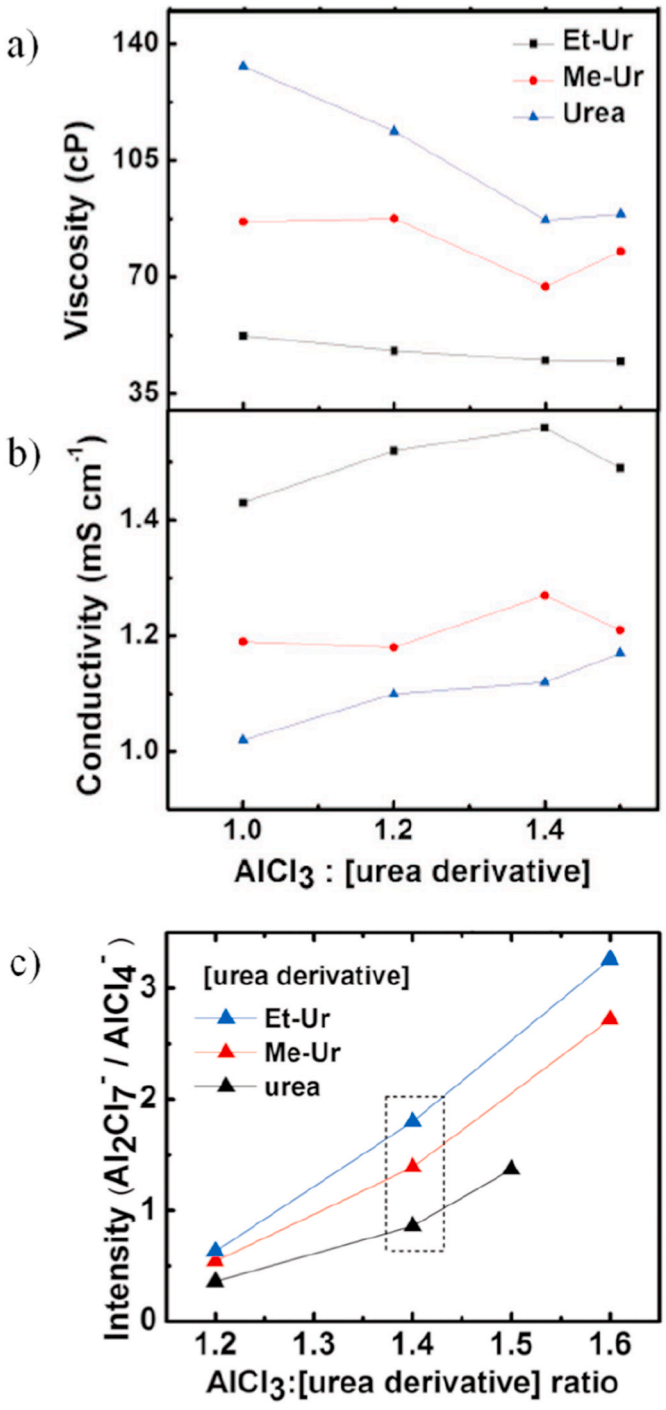

Fig. 4. Graphical presentation of the viscosities (a) and conductivities (b) of $AlCl_3$/[urea derivative] = 1.0, 1.2, 1.4, 1.5 DES electrolytes at 25 ± 1 °C. (c) Raman intensity ratios of $Al_2Cl_7^-$ to $AlCl_4^-$ for different urea derivatives at certain $AlCl_3$/[urea derivative] ratios [177].

derivatives of urea (*N*-methyl urea and *N*-ethyl urea) [177] mixed with $AlCl_3$ to obtain an electrolyte with lower viscosity and higher conductivity than the urea-based electrolyte. The investigated electrolytes had viscosity values of $\eta = 45$, 67, and 87 cP for *N*-ethyl urea, *N*-methyl urea, and urea, respectively, at 25 °C and mole ratios of 1.4 (Fig. 4a). The conductivities were $\sigma = 1.56$, 1.24, and 1.12 mS cm^{-1} for the *N*-ethyl urea, *N*-methyl urea, and urea electrolytes, respectively, at 25 °C and mole ratios of 1.4 (Fig. 4b). Additionally, the urea analog-based electrolytes showed different discharge voltages in AGDIB cells (2.04 and 2.08 V for *N*-methyl urea and *N*-ethyl urea electrolytes, respectively, vs. 1.95 V for urea the system at a specific current of 100 mA g^{-1} with ≈ 5 mg cm^{-2} mass loading), due to changes in the concentrations of ionic species. The ionic speciation of the different electrolytes investigated by Raman spectroscopy suggested that the formation of new $AlCl_4^-$ ions became less favorable when Me-Ur and Et-Ur were used, as the $AlCl_3$ being added to the system was coupling to $AlCl_4^-$ to form more $Al_2Cl_7^-$ ions (Fig. 4c) [177]. The group used operando Raman spectroscopy performed during cyclic voltammetry to show that aluminum deposition occurred directly through the reduction of $Al_2Cl_7^-$, indicating that the $[AlCl_2{\cdot}(urea)_n]^+$ cations did not have a role in the deposition process [177].

Bian et al. [218] evaluated the use of $AlCl_3$/urea DES electrolytes for Al/S battery applications, proved beneficial in terms of cycle life and improved discharge voltage plateau (~1.8 V). The fundamental parameter that caused the superior performance was identified to be the lower solubility of sulfur in the $AlCl_3$/urea DES electrolyte compared to the conventional $AlCl_3$/EMIM electrolyte. However, considering that the reaction of an Al/S system is expected to follow the conversion reaction (8):

$$2Al^{3+} + 3S + 6e^- \leftrightarrow Al_2S_3 \quad (8)$$

From the ΔG_0 of formation of Al_2S_3 at 298.15 K (ΔG_0 = -153.0 kcal/mol) [219,220], we can calculate that the ΔE_0 of the reaction is equal to 1.12 V. The superior working voltage reported by Bian et al. [218] most likely indicates a different reaction pathway, suggesting the possible insertion of $AlCl_4^-$ into the multi-walled carbon nanotubes used in the cathode. The use of DES based electrolytes for Al/S system was recently studied by Chu et al. [180], who employed $AlCl_3$/acetamide for reversible room-temperature Al–S batteries. The reported results showed an initial capacity above 1500 mA h g^{-1} and good rate performance. DFT studies suggested that the presence of $[AlCl_2(acetamide)_2]^+$ ions led to an energetically favorable reaction pathway, justifying the superior performance in comparison to the conventional $AlCl_4^-$ based electrolyte. Lampkin et al. [86] reported a detailed comparison of acetamide and urea DESs with conventional EMIMCl:$AlCl_3$ electrolytes for Al/S batteries. Their report identified that the high viscosity of urea and acetamide electrolytes is one of the most critical factors affecting the performance of electrodes with high sulfur loading. This in agreement with the findings of Dai's group for Al/graphite battery systems [177].

4.1.2. Cell component stability in chloroaluminate electrolytes

The most critical aspect of chloroaluminate electrolytes is their elevated reactivity and corrosivity. Most of the metals suitable for current collectors or cell components are corroded by chloroaluminate electrolytes, including carbon steel (CS), 304 stainless steel (304 SS), and pure titanium (Ti) [221–226]. The reactivity of chloroaluminate with cell components and the use of stable metals as current collectors are essential parameters for producing reliable results from electrochemical systems. In 2013, Reed et al. [227] clearly demonstrated the role of stainless steel when it used as a current collector in chloroaluminate systems by showing that the voltage behavior reported in the tested Al/V_2O_5 cell can be attributed to the dissolution and shuttling of the iron and chromium ions contained in the stainless steel current collector. However, several studies have used unstable metals as current collectors in combination with chloroaluminate melt electrolytes. Guo et al. [228] reported an overview of the implications of using highly reactive chloroaluminate electrolytes for Al-battery applications. Their study showed the importance of selecting a proper cell configuration to perform electrochemical tests, and that the use of an unstable current collector can generate false discharge capacities (Fig. 4 a-f). Their study indicated that molybdenum and glassy carbon are suitable current collector materials. However, these materials are not suitable for large-scale battery production. An alternative current collector has been proposed by Kovalenko and co-workers [229]; they proposed a flexible current collector fabricated by coating TiN on stainless steel or flexible polyimide substrates by using low-cost, rapid, scalable methods such as magnetron sputtering. The use of the TiN coated current collector increased the cathodic operation voltage limit up to 2.5 V versus Al^{3+}/Al, superior to the conventional current collectors used for Al-battery system (Fig. 5g-e). Moreover, the alternative current collector was successfully integrated into an AGDIB that had a high coulombic efficiency of 99.5% and a cyclability of more than 500 cycles.

The elevated reactivity of chloroaluminate is also critical for cathode materials. Guo et al. [230] recently reported a detailed investigation on the chemical stability of V_2O_5 in neutral and acidic EMIMCl:$AlCl_3$ melts. The study showed that V_2O_5 reacts in the acidic melt to form $VOCl_3$ and amorphous Al_2O_3, while in neutral melts, V_2O_5 and $AlCl_4$ react to form VO_2Cl and $AlCl_3VO_3$. The formed soluble products are electrochemically active with reversible redox reactions between V^{5+} and V^{2+} oxidation states. Indeed, the Al/V_2O_5 cell shows a charge/discharge behavior that is most likely associated with the redox reaction of the solubilized degradation products. Their study raises questions on the chemical stability of other Al-ion positive electrode materials in chloroaluminate ionic liquid electrolytes. Considering that the Al stripping/deposition process is guaranteed by the ability of chloroaluminate to dissolve the Al_2O_3 passivation layer and that Al_2O_3 is one of the more stable metal oxides [231], one can infer that the number of chemically stable metal oxide cathodes is limited. An additional critical point of chloroaluminate-based systems is the reactivity of chloroaluminate with the polymers used as separators and polymeric binders in batteries. Elia et al. [232] screened the chemical stability of a series of separators conventionally employed for Li-ion battery application against chloroaluminate melts. Their study showed the instability of conventional polymers, including polypropylene, polyethylene, poly(vinyl alcohol), and polyimide, thus limiting the choice of suitable candidates for the fabrication of cells. The study indicated that polyacrylonitrile (PAN) was stable. The polymer was used to fabricate PAN membranes constituted of nonwoven fibers, successfully integrated into AGDIBs. Moreover, the PAN separator showed better compatibility and improved aluminum interface stability, which positively affected the aluminum dissolution/deposition process. Investigations of suitable cell components characterized by good stability in chloroaluminate melts are one approach. On the other hand, some research has been dedicated to reducing the reactivity and corrosivity of chloroaluminate-based systems while keeping the Al stripping/deposition properties. Nakayama et al. [233] screened various ternary electrolyte compositions including aluminum chlorides, dialkylsulfones, and dilutants (toluene, benzene, acetone, THF, GBL), and found that an $AlCl_3$/di-n-propyl sulfone (EnPS)/Toluene 1/0.7/2.9 (mole ratio) system guaranteed efficient Al stripping/deposition and had reduced corrosivity against stainless steel (SUS). Li et al. [182] proposed a 4-ethylpyridine/$AlCl_3$ deep eutectic solvent (DES) that had limited corrosivity against Al, Cu, and Ni. Additionally, their report demonstrated that the electrolyte was capable of operating in ambient atmosphere and reported an AGDIB cycling test conducted in open air. However, for both reports, the stability of the investigated metals was investigated only from the chemical point of view, and no electrochemical corrosion tests were reported.

4.1.3. Polymer electrolytes

An alternative approach to limit the reactivity and corrosivity of chloroaluminate is their inclusion in a polymer in the form of a gel

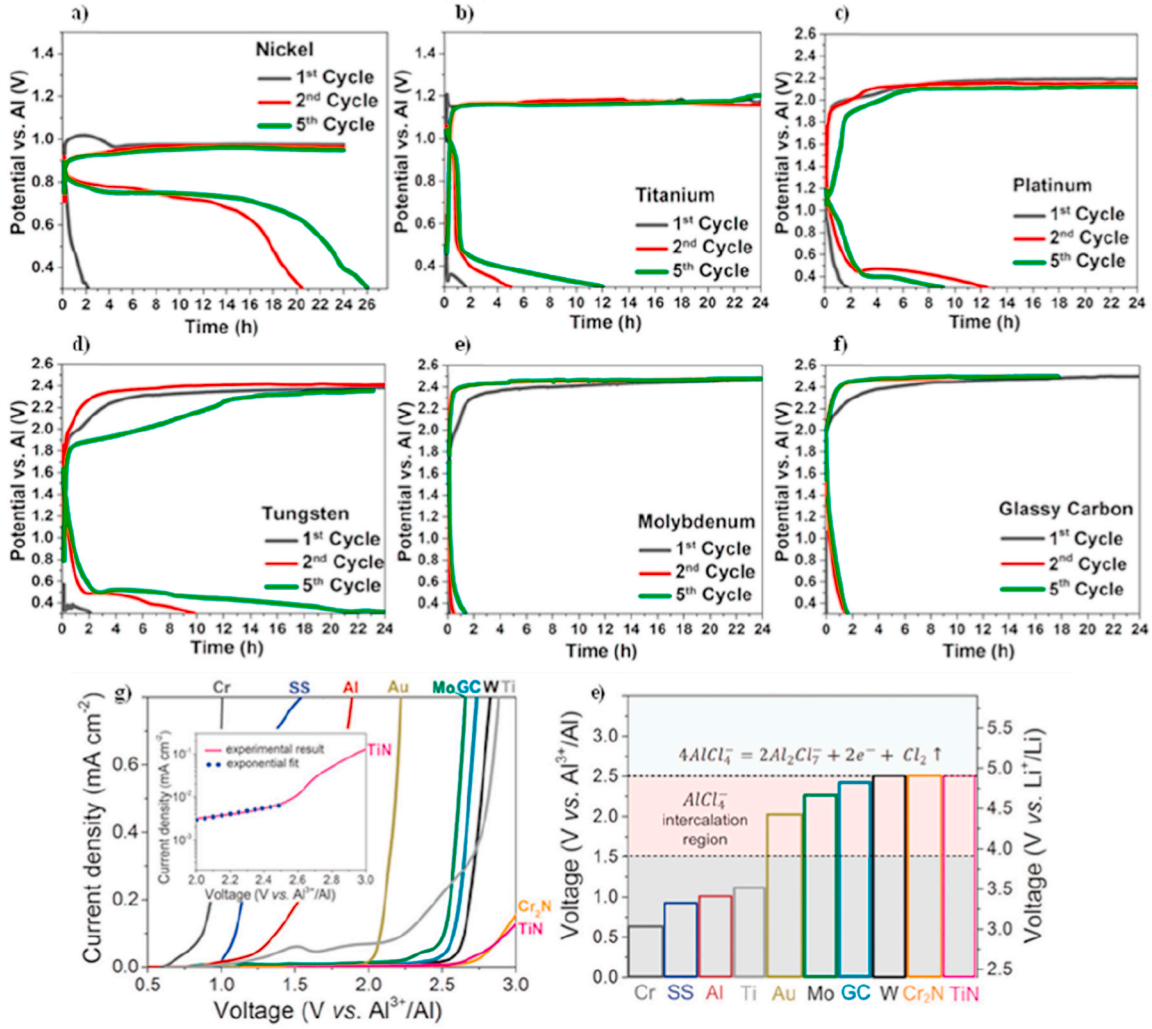

Fig. 5. Galvanostatic discharge−charge (reduction−oxidation) curves of various conductive substrates including (a) nickel, (b) titanium, (c) platinum, (d) tungsten, (e) molybdenum, and (f) glassy carbon versus aluminum under a current of 1.78 × 10^{-2} mA cm^{-2} at room temperature using an aluminum chloride–1-ethyl-3-methylimidazolium chloride ionic liquid (IL) electrolyte. (g) Cyclic voltammetry curves for various current collectors measured in $AlCl_3$-[EMIM]Cl (r = 2) at a rate of 10 mV s^{-1} (inset: current–potential relationship of the TiN current collector on a logarithmic scale). (h) Illustration of the oxidative stabilities of various current collector materials in $AlCl_3$-[EMIM]Cl (r = 2) in terms of the voltage versus Al^{3+}/Al and Li^+/Li.

polymer electrolyte [186–191]. The confinement of the reactive melt in the polymer matrix is expected to mitigate the reactivity and corrosivity issues. Sun et al. [186] investigated a gel polymer electrolyte prepared via free-radical polymerization of a mixture of acrylamide monomer and EMIMCl:$AlCl_3$, and showed that the gel polymer electrolyte could maintain its activity after exposure to air. Yu et al. [189] followed a similar approach, using dichloromethane as the solvent during the polymerization process of acrylamide and obtaining a gel polymer electrolyte containing the EMIMCl:$AlCl_3$ electrolyte that was directly cast on the Al anode by solvent casting. The gel electrolyte was tested in an AGDIB and showed good stability and the ability to operate at low temperature (−10 °C). Additionally, the authors demonstrated that the cell configuration was capable of operating upon exposure to air. Moreover, a comparison of the gas generation of Al/graphite cells using the gel polymer electrolyte and the conventional liquid EMIMCl:$AlCl_3$ system showed there was higher hydrogen generation for the liquid electrolyte. The same group evaluated [190] the use of triethylamine hydrochloride (Et_3NHCl) as an alternative to the EMIMCl for the preparation of gel polymer electrolytes, which showed superior performance in AGDIBs with stable cycling extending to more than 800 cycles. The improved performance of the Et_3NHCl based gel polymer electrolyte was attributed to the superior stability of the anodic electrochemical window.

4.1.4. Chlorine-free electrolyte

The ideal solution to the reactivity of chloroaluminate is to substitute chloroaluminate electrolytes with an alternative Cl-free electrolyte. However, this is not an easy task since the efficient Al stripping/deposition process is guaranteed in acidic melts by the presence of the dimeric $Al_2Cl_7^-$ [206–211] and by the removal of the Al_2O_3 passivation layer [193,210]. Johansson's group has obtained some preliminary results in this direction, demonstrating a chlorine-free system based on acylamino group solvents (urea, acetamide, and their derivatives) combined with highly dissociative salts based on charge delocalized weak Lewis basic anions $Al(CF_3SO_3)_3$ [195], and coordination metal complexes obtained from anion metathesis reactions ([Al(1-butylimidazole)$_6$][bis(trifluoromethanesulfonyl)-imide]$_3$) [196]. They showed that by employing a ternary mixture of aluminum trifluoromethanesulfonate (Al[TfO]$_3$), *N*-methylacetamide (NMA) and urea [195] (Al[TfO]$_3$/NMA/urea molar ratio of 1:15:4), the dissociation state of Al[TfO]$_3$ drastically changes, most likely due to the unique coordination environment of dissolved Al^{3+} ions. The electrolyte solution showed a wider electrochemical stability window than conventional $AlCl_3$:[EMIM]Cl and had satisfactory activity for the electrochemical

dissolution/plating of aluminum. The reduced electrochemical activity was compensated by the lower reactivity of the electrolyte, demonstrating that the selection of the proper electrolyte can enable reversible electrochemical stripping/plating process of aluminum in non-corrosive electrolytes. However, the development of a chlorine-free electrolyte with the proper ionic speciation does not guarantee reversible stripping/plating, since the Al/electrolyte interface also limits the process. Indeed, it has been recently shown that it is possible to artificially form a suitable interphase that enables the Al stripping/deposition process in chlorine-free systems [28,193]. This "artificial interphase" can be created by treating the Al-metal with the conventional chloroaluminate, thus leading to partial removal of the Al_2O_3 passivation layer, and the formation of a layer rich in Al, Cl, and N at the surface [28]. The suitability of this concept for use in Al-batteries has been reported using 1-butyl-3-methylimidazolium trifluoromethanesulfonate $BMIMCF_3SO_3$–$Al(CF_3SO_3)_3$ and a "water-in-salt" electrolyte (3 M $Al(CF_3SO_3)_3$ in H_2O [28,30,192]).

4.2. Cathodes for non-aqueous Al-batteries

The diffusion of multivalent cations suffers from poor kinetics due to the higher electrostatic interactions when compared to monovalent Li-ions [234]. The trivalent Al^{3+} ion induces several kinetic issues:

i) Strong electrostatic interactions

In a typical ion diffusion process inside a bulk solid, the inserted ions must overcome the repulsive forces from lattice metal cations and also the attractive forces from the lattice anions. Usually, ions of higher charge density encounter stronger electrostatic interactions that impair ionic diffusion.

ii) Difficult charge compensation

Ion diffusion is accompanied by the redistribution of charges to reach local electroneutrality. In a mixed conductive solid cathode, charge compensation can be reflected by the valence change of the lattice metal cations (or/and the anions). To insert one Al^{3+} per formula unit, 3 electrons are accepted by the metal redox center, meaning a reduction of three valence states. For a conventional cathode material, it is generally not easy to tolerate such a massive injection of electrons. Furthermore, the substantial valence change alters the cation radius resulting in massive lattice structural changes. To mitigate this issue, the majority of non-aqueous Al-battery technologies exploit the $AlCl_4^-$ anion in the electrochemical process and not Al^{3+}. Accordingly, it is possible to classify the cathodes employed in non-aqueous Al-battery technologies as dual ion cathodes (graphite, organic) or rocking chair cathodes (sulfur, MnO_2).

Additionally, an important aspect to take into account is the chemical stability of the cathode materials in acidic chloroaluminate melts [230]. As shown recently by Guo et al. [230], V_2O_5 cathodes degrade in neutral and acidic $EMIMCl:AlCl_3$ melts forming electrochemically active soluble products (see electrolyte section). The implications of this issue raise questions about the suitability of chloroaluminate as an electrolyte for metal oxides and metal sulfides, where the chemical stability must be verified before electrochemical tests are performed to avoid misleading results.

Considering this fundamental aspect, the following section of the review focuses on electrode materials that have been proven to be chemically stable in chloroaluminate melts, like graphite or organic cathodes (Table 3, Fig. 6). Additionally, a section is dedicated to the Al/S system, where the formation of soluble electrochemically active reaction products is expected.

Table 3
List of cathodes chemistry obtained from a survey of 106 Al-battery related papers.

Cathodes chemistry	References
Carbon/Graphitic cathodes	[10,13,88,90–98,100–109,111–113,115,160–162,167,168,229,232,235–248]
Sulfur cathodes	[79–86,165,180,249–251]
Organic/polymeric cathodes	[146–151,252]
Metal sulfide	[123–131,133–142,173,253,254]
Metal Oxide	[52,74,153,156–158,184,230,255,256]
I_2	[119,120]
Metal Chloride	[89,183]
MXene	[144,145,257]

4.2.1. Dual-ion cathodes

4.2.1.1. Graphite cathode

4.2.1.1.1. Working principle of AGDIBs. Aluminum graphite dual-ion batteries (AGDIBs) operate through the oxidation of the graphite structure at the positive side of the battery along with the intercalation of $AlCl_4^-$ ions between graphene layers. The intercalation process follows a staging mechanism with the formation of graphite intercalated compounds (GICs) [258,259]. Fig. 7a reports the operando energy-dispersive diffractions (ED–XRD) of an AGDIB battery employing natural graphite (NG) as a positive electrode and $EMIMCl:AlCl_3$ 1:1.5 as the electrolyte [260]. The spectra evolution upon cycling reveals the disappearing of the (002) peak characteristic of graphite (at 35.5 keV), followed by the formation of new peaks, indicating the formation of a graphite intercalation compound (GIC) [10,117,161,179,258,259]. The electrochemical process is entirely reversible, as demonstrated by the reappearing of the initial (002) peak. On the negative side, concomitant plating/stripping of aluminum occurs from chloroaluminate-based ionic liquid melts. The working mechanism of AGDIBs (Fig. 7b) can be described by the following half-reactions occurring during charging of the battery:

On the negative side:

$$4Al_2Cl_7^- + 3e^- \leftrightarrow 7AlCl_4^- + Al \quad (9)$$

On the positive side:

$$xC + AlCl_4^- \leftrightarrow C_x\left(AlCl_4^-\right) + e^- \quad (10)$$

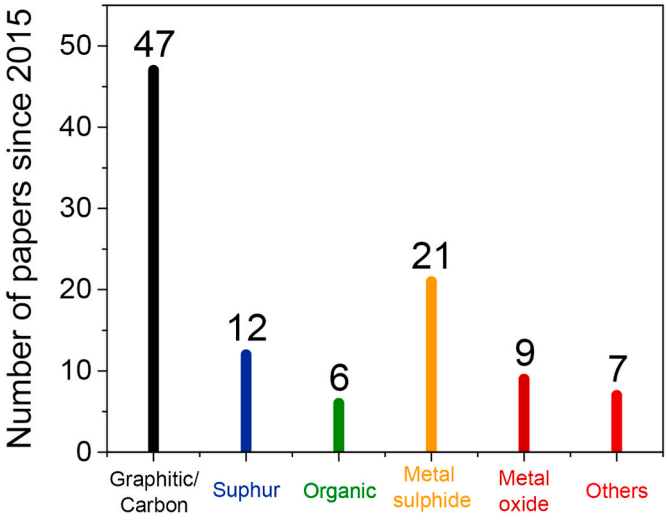

Fig. 6. Number of papers since 2015 dealing with Al-based rechargeable batteries using carbon/graphitic, sulfur, organic/polymeric, metal sulfide, metal oxide, metal chloride, I_2, and MXene cathode chemistry. The survey was done using the papers listed in Table 3. (last updated on May 1, 2020). The keyword used for the search in Scopus were "Aluminum battery".

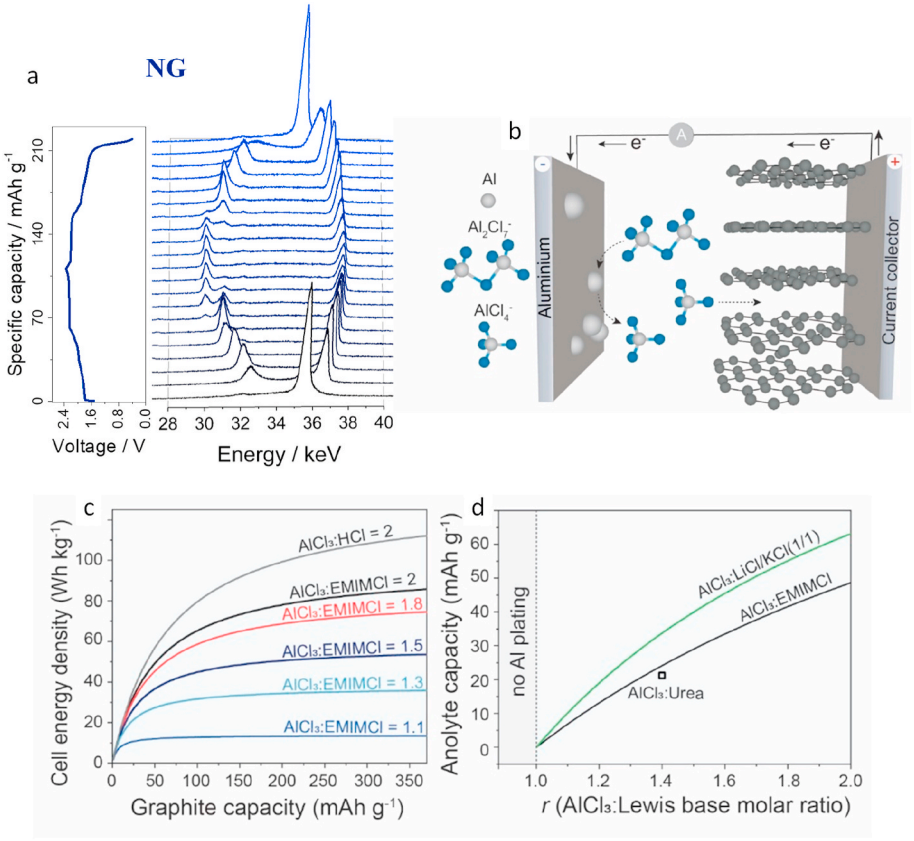

Fig. 7. (a) Operando energy-dispersive diffraction (ED–XRD) of a Al/EMIMCl:$AlCl_3$/NG cell cycled at 25 mA g^{-1} current density and room temperature. The ED–XRD curves were displaced vertically for clarity. The voltage profile recorded during the test is reported along with the ED–XRD spectra. The ED–XRD spectra are placed along the voltage plateau, corresponding to the cycling-specific step. Adapted from Ref. [260] Wiley (b) Schematic of the charging process for an AGDIB. Adapted from Ref. [105], ACS (c) Comparison of cell-level energy densities vs capacity of graphite for different anolyte acidities. The curves were computed from Eq. (1). The average discharge voltage was assumed to be equal to 2 V. Adapted from Ref. [95], ACS (d) The capacity of different aluminum anolytes versus their acidity (r). The curves were computed from Eq. (7). The point for $AlCl_3$-Urea anolyte is derived from the concentration of $Al_2Cl_7^-$ ions in $AlCl_3$-Urea reported in Refs. [178].

Chloroaluminate ionic liquids can be defined as a mixture of $AlCl_3$ and other Cl-based salts, such as 1-butyl-3-methylimidazolium chloride (BMIMCl) [261,262], 1-ethyl-3-methylimidazolium chloride (EMIMCl) [10,13,95,98,110,147,153,162,229] and others [162,164]. Owing to the acid-base reaction between $AlCl_3$ (Lewis acid) and Cl^- (Lewis base), the mixture turns liquid at room temperature (named room temperature ionic liquids, RTILs), forming $AlCl_4^-$ anions which are charge-balanced with, for instance, $EMIM^+$ cations. The excess of $AlCl_3$ relative to EMIMCl results in the formation of acidic ionic liquids containing $Al_2Cl_7^-$ ions. Aluminum electroplating from chloroaluminate based ionic liquids was comprehensively examined in the past, pointing to the fact that the electroplating of Al takes place only in acidic formulations (in the presence $Al_2Cl_7^-$, but not $AlCl_4^-$ ions) [205,207,208,210,214,215,263–266]. Therefore, in the case where there is an excess of EMIMCl compared to $AlCl_3$ (neutral or basic melts), aluminum cannot be deposited. In this regard, the quantity of $Al_2Cl_7^-$ ions, and therefore the volume/mass of the aluminum ionic liquid, should be equilibrated with the capacity of the graphite. For every three $AlCl_4^-$ anions intercalated into the graphite, one aluminum atom is simultaneously electrodeposited. Consequently, the charging process stops when only $AlCl_4^-$ ions are left in the chloroaluminate melt, corresponding to the formation of a neutral melt ($AlCl_3$:EMIMCl = 1) or when the highest capacity of the graphite is reached. The uppermost molar ratio (r) between $AlCl_3$ and EMIMCl that still forms a liquid is *ca.* 2:1. At higher ratios, $AlCl_3$ exists in the form of a precipitate. As follows from the mechanism of AGDIBs, it should also be noted that starting with an Al anode is not a necessity because any current collector with a thin Al film as a seed layer for the initial electroplating of Al would be sufficient. Notably, in AGDIBs, there is no unidirectional current of Al^{3+} ions, or any other Al ions, from the positive to the negative electrodes during charging, which is implied in "rocking-chair" Al-ion batteries. Therefore, it is not correct to name AGDIBs "Al-ion batteries". The operating principle is substantially different from the mechanism of metal-ion batteries: during the charging process, Al ions are consumed from the chloroaluminate melt and are being taken up by both the negative and positive electrodes (Fig. 7b).

Taking into consideration the mass/volume of the ionic liquid, the theoretical charge-storage capacity of an AGDIB on a cell level can be calculated using the following equations that include the masses of both the graphite and the chloroaluminate melt:

$$\text{Gravimetric } C_{cell} = \frac{Fx(r-1)C_c}{Fx(r-1) + C_c\left(rM_{AlCl_3} + M_{XCl}\right)} \ \left(\text{mAh g}^{-1}\right) \tag{11}$$

$$\text{Volumetric } C_{cell} = \frac{Fx(r-1)C_c\rho}{Fx(r-1) + C_c\left(rM_{AlCl_3} + M_{XCl}\right)} \ \left(\text{mAh mL}^{-1}\right) \tag{12}$$

where $x = \frac{3}{4}$ (mol amount of electrons required to reduce 1 mol of $Al_2Cl_7^-$ ions), M_{AlCl_3} is the molar mass of $AlCl_3$ in g mol^{-1}, M_{XCl} is the molar mass of the Cl^- source [for example 1-butyl-3-methylimidazolium chloride, 1-ethyl-3-methylimidazolium chloride or any other Cl^- source (i.e. HCl)] in g mol^{-1}, r is the $AlCl_3$:XCl molar ratio and ρ is the density of the chloroaluminate ionic liquid in g mL^{-1}. To assess the practical capacity of AGDIBs, C_{total} should be further reduced by 25–50% by taking into consideration the weight of separators, current collectors, and packaging (depending on the battery design).

The impact of the acidity r of a chloroaluminate melt on the theoretical energy density of AGDIBs is shown in Fig. 7c using calculations equation (11) with the assumption that the voltage of the AGDIB is equal to 2 V regardless of the acidity. The discharge voltage of 2 V is the highest reported voltage value that was experimentally measured at r = 1.3. According to Fig. 7d, apart from the graphite capacity, the acidity r of the chloroaluminate ionic liquid defines to a large extent the energy density of AGDIBs. The relationship between the acidity r of chloroaluminate ionic liquids and their theoretical capacity can be shown as follows:

$$\text{Gravimetric } C_{an} = \frac{Fx(r-1)}{rM_{AlCl_3} + M_{XCl}} \ \left(\text{mAh g}^{-1}\right) \quad (13)$$

$$\text{Volumetric } C_{an} = \frac{Fx(r-1)\rho}{rM_{AlCl_3} + M_{XCl}} \ \left(\text{mAh g}^{-1}\right) \quad (14)$$

For instance, for $r = 2$ and $r = 1.3$, the gravimetric and volumetric capacities of an $AlCl_3$:EMIMCl ionic liquid is equal to 48 mA h g^{-1}, 63 Ah L^{-1}, and 19 mA h g^{-1}, 24 Ah L^{-1}, respectively. Consequently, to achieve the highest energy density for AGDIBs, both the capacity of the cathode (C_c), and the acidity r of the ionic liquid should be maximized. Notably, we examined all reported data on AGDIBs [10,13,88,90,93–95,100,102,103,106,107,111,112,115,167,229,236,241–248] and identified that the highest experimental energy density of *ca.* 65 Wh kg^{-1} was reported for AGDIBs composed of kish graphite flakes with a capacity of 142 mA h g^{-1} (discharge voltage of 1.79 V) and an $AlCl_3$:EMIMCl ionic liquid with $r = 2$ [98]. It should be noted, however, that the majority of reports on AGDIBs are based on chloroaluminate ionic liquid melts with rather low acidity, $r = 1.3$. This causes severe limitations on the energy density of AGDIBs, not exceeding 30 Wh kg^{-1}.

Importantly, apart from conventional room-temperature ionic liquids, AGDIBs can be operated using other chloroaluminate formulations such as $AlCl_3$/NaCl [248,267] or $AlCl_3$/LiCl/KCl [248,268] fully inorganic melts as cost-efficient alternatives. In this respect, because of the lower molar mass of alkali chlorides, their theoretical charge storage capacity is higher than RTILs of the same acidity (Fig. 7d). Besides the high capacity and low-cost, inorganic molten salts have low viscosity and high ionic conductivity at melting temperatures that enhance the kinetics of the $AlCl_4^-$ insertion/de-insertion process in the graphite. We have to stress that in the context of large-scale industrial applications of AGDIBs composed of inorganic molten salts, their high melting points are not considered a disadvantage because the working temperature of AGDIBs can be supported by Joule heating being produced during the charge/discharge cycles and by the heat produced from industrial processes.

In addition to RTILs and fully inorganic melts, deep eutectic solvents (DESs), were recently examined as Al electrolytes for AGDIBs [214,265,269]. Similar to RTILs [264], DESs can be described as liquids composed of a metal halide (Lewis acid) and an oxygen donor amide (Lewis base), such as Urea. Consequently, $AlCl_3$-Urea DESs can be formed by the exothermic reaction between $AlCl_3$ and Urea as follows:

$$2AlCl_3 + 2Urea \rightarrow AlCl_4^- + [AlCl_2(Urea)_2]^+ \quad (15)$$

In-depth investigations of DESs using NMR [174,177,270] and Raman [176–178,270] spectroscopy have shown that $AlCl_3$-Urea DES formulations with an $AlCl_3$/Urea molar ratio equal to one are composed of $AlCl_4^-$ anions. When the acidity of $AlCl_3$-Urea melts increases, the amount of $Al_2Cl_7^-$ ions progressively increases in comparison to the quantity of the $AlCl_4^-$ ions. The highest acidity (r) of $AlCl_3$-Urea DESs that can be experimentally achieved is $r \approx 1.5$ [177]. Notably, it has been shown that Al electrodeposition from $AlCl_3$-Urea DESs occurs only in acidic formulations ($AlCl_3$/Urea > 1.1) with concomitant decreases and increases of the concentrations of $Al_2Cl_7^-$ and $AlCl_4^-$ ions, respectively [178]. The same finding has also been observed for other $AlCl_3$-amide DESs [271]. Therefore, like RTILs, Al electroplating/stripping in $AlCl_3$-Urea DESs occurs as follows:

$$4Al_2Cl_7^- + 3e^- \leftrightarrow 7AlCl_4^- + Al \quad (16)$$

From this perspective, the theoretical charge storage capacity of an $AlCl_3$-Urea melt at $r \approx 1.4$ can be estimated to be in the range of 20–21 mA h g^{-1}, using the concentration of $Al_2Cl_7^-$ ions in $AlCl_3$:Urea DES reported in Refs. [178]. Similar capacities of *ca.* 16 mA h g^{-1} and 18 mA h g^{-1} can be calculated for $AlCl_3$:Me-Urea and $AlCl_3$:Et-Urea melts, respectively.

Although the theoretical capacities of chloroaluminate melts allow the assessment of the energy density of AGDIBs, it should be noted that those capacities are not always achievable experimentally. Recently, Kravchyk et al. [105] pointed out that the capacity of ionic RTILs depends on the current density and on whether the $Al_2Cl_7^-$ ions can be fully depleted from the ionic liquid melts upon Al electrodeposition. In order to unveil the limitations of chloroaluminate ionic liquid electrolytes, Kravchyk et al. [105] measured AGDIBs in three-electrode configurations with a significant excess of graphite cathode. The voltage profiles at the positive (graphite), and negative (aluminum) electrodes were monitored with Al foil acting as the reference electrode (Fig. 8a and b). These electrochemical measurements have shed light onto two issues. First, as foreseen, higher charge storage capacities for RTILs can be achieved only for highly acidic melts. As an example, the gravimetric capacity of an $AlCl_3$:EMIMCl ionic liquid with $r = 1.3$ was *ca.* 21 mA h g^{-1} at a current density of 20 mA g^{-1}. On the contrary, the capacity was *ca.* 46 mA h g^{-1} at $r = 2$. These findings demonstrate that the highest energy density AGDIBs can be reached by employing chloroaluminate ionic melts with $r = 2$. Consequently, future research on AGDIBs should be performed with the highest acidity formulations. Secondly, the current density has a profound effect on the capacity of chloroaluminate ionic liquids. The latter effect is apparent when there is a substantial deviation of the voltage of the negative electrode from 0 V *vs.* Al^{3+}/Al at high current densities. Consequently, minor capacities were obtained at high current densities of 1 A g^{-1} (*ca.* 10–14% of the theoretical values, Fig. 7c). In light of these results, significant deviations in the energy densities of real AGDIBs are expected from the theoretical energy densities of AGDIBs.

4.2.1.1.2. Electrochemical performance of graphite in AGDIBs

4.2.1.1.2.1. Structural aspects of graphite

Aiming to enhance the charge storage capacity and voltage of graphite positive electrodes in AGDIBs, recent experimental endeavors have focused on diverse types of natural and synthetic graphite [10,13,88,90,93–95,100,103,106,111,112,115,167,229,235,236,241,243–246,248].

In this section, we extensively explore the major structural and morphological aspects of graphite and their implications on the electrochemical performance of AGDIBs.

Overall, the structure of the graphite can be characterized by two primary factors, namely, the graphitization degree (GD) and the perfection of the graphite structure (PGS). GD represents the degree of non-graphitic carbon that has been converted into graphitized carbon. In fact, this factor is frequently used to assess the graphitization level of amorphous carbon following heat-treatment. In accordance with the relationship suggested in Refs. [272], the GD can be computed from the following formula:

$$GD\ (\%) = \frac{0.3440 - d_{(002)}}{0.3440 - 0.3354} \times 100 \quad (17)$$

where 0.3440 nm is the graphene-graphene interlayer distance in a non-graphitized structure, 0.3354 nm is the graphene-graphene interlayer distance of a pure graphite structure, and $d_{(002)}$ is the interlayer distance measured from XRD patterns of the studied carbon material.

Examples of carbonous materials with high GD approaching 100% include vein graphite and natural graphite flakes. The GD of synthetic graphite materials is heavily dependent on the synthesis conditions. For instance, artificial graphite can have a highly anisotropic structure approaching the GD of a single crystal. Graphite manufactured by carbon crystallization from molten steel during the steel manufacturing process (kish graphite), the pyrolysis of gaseous hydrocarbons (pyrolytic graphite) and petroleum coke (synthetic graphite flakes) possess the highest GDs among artificially made graphite materials. However, the majority of artificially produced graphites are characterized by low anisotropy levels. It should be mentioned that the shape of the particles of a graphite reflects its GD. Graphite with the highest GD tends to have a well-defined flake-like morphology.

PGS can be defined as perfection in the ordering of carbon atoms

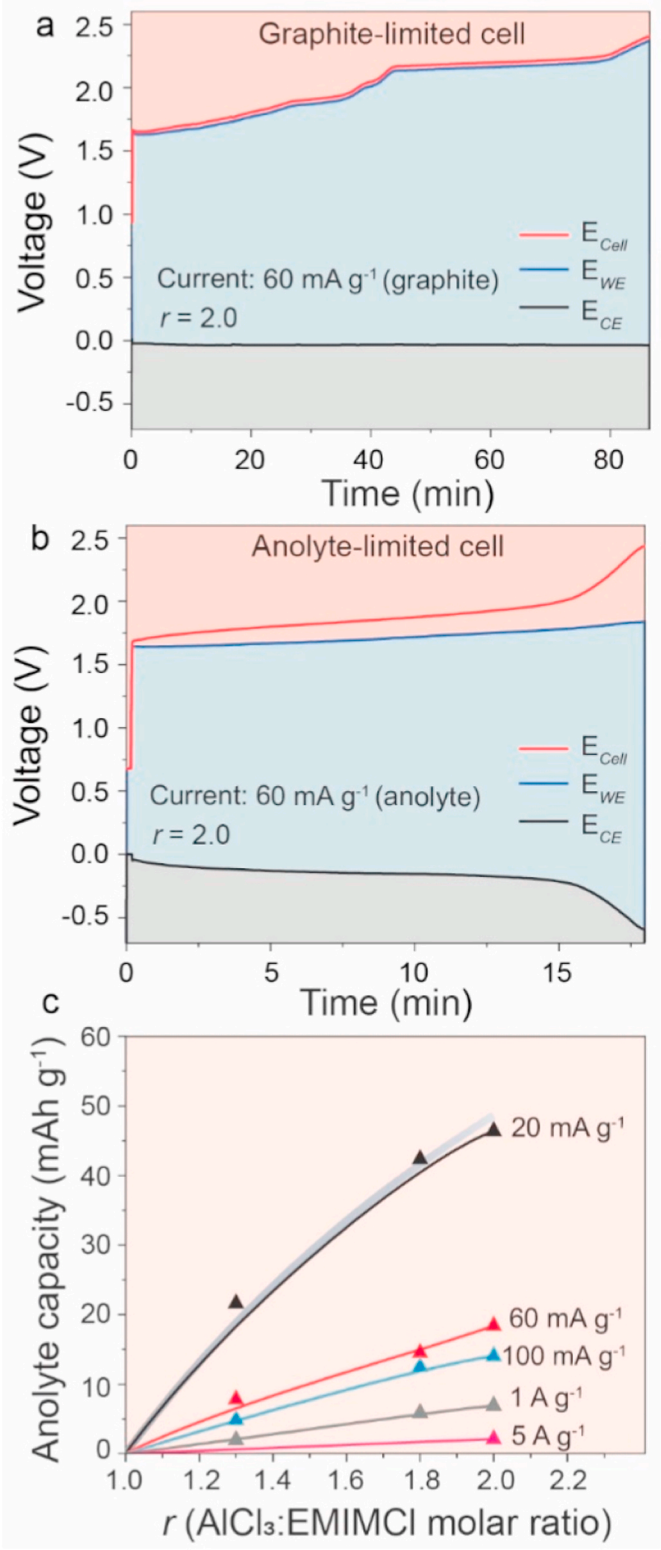

Fig. 8. (a, b) Galvanostatic charge voltage profiles for a chloroaluminate anolyte (E_{CE}; $AlCl_3$:EMIMCl; r = 2), graphite (E_{WE}), and a full cell (E_{Cell}) measured versus an Al foil reference electrode in (a) graphite-limited and (b) anolyte-limited cell configurations. (c) Charge storage capacities of the chloroaluminate anolyte with r = 1.3, 1.8, and 2.0 measured at different current densities. The grey line indicates the theoretical charge storage capacity of the anolyte computed from Eq (1). Adapted from Ref. [105] ACS.

yielding a low concentration of impurities and structural disorders and defects, including prismatic edge dislocations, prismatic screw dislocations, non-basal edge dislocations, and basal dislocations. Generally, high PGS graphites have the smallest interplanar distance deviations from the value of 0.3354 nm, large crystallites, and the lowest levels of the various defects, which can be simply identified using X-ray diffraction (XRD) and Raman spectroscopy, respectively [273–275]. For instance, in respect to the Raman spectroscopy measurements, the intensity ratio of the D to G bands (I_D/I_G ratio) is frequently used for assessing the defectiveness of the graphite structure and for measuring the average concentration of defects present in the basal plane of graphite and at the edge plane surfaces.

The impact of the diverse types of graphite with different GDs and PGS on the electrochemical performance of AGDIBs has recently been assessed by Wang et al. [98] Specifically, it was shown that kish graphite flakes, potato-shaped graphite particles, and amorphous carbon have substantial differences in performance (Fig. 9a). Kish graphite flakes, which had the smallest interplanar d-spacing and the lowest D-band intensity, demonstrated the highest capacity of 130 mA h g^{-1} (Fig. 9b, c). On the contrary, the potato-shaped graphite particles with low structural quality showed much lower charge storage capacity. Finally, amorphous carbon exhibited the smallest capacity along with sloppy galvanostatic voltage curves. In fact, $AlCl_4^-$ storage in amorphous carbon appears to be analogous to the insertion of Li^+ ions into hard carbon, where its capacity is spread over a broad voltage range [276]. Following reports of Wang et al. [98], Dai et al. [13,93,106,174,179] and others [104,114,277], it can be concluded that the charge storage capacity and voltage associated with the intercalation of $AlCl_4^-$ ions into graphitic structures are very much dependent on the nature of the graphite, which can be represented in a simplified fashion by the GD and PGS of the graphite.

4.2.1.1.2.2. Impact of the particle size and morphology of graphite on electrochemical performance

In addition to the structural factors, the morphology and particle size of the graphite has substantial impact on the electrochemical performance of graphite. For instance, Kravchyk et al. [95] found that the charge storage capacity of large-sized natural graphite flakes can be increased after the graphite flakes are sonicated into micron-sized flakes. Such processing methods preserve the GD and PGS of the graphite. Other types of top-down mechanical processes, such as ball-milling, yield partial amorphization of the graphite. Notably, the employment of small natural GF and processed large GF of the same size does not necessarily lead to similar results, suggesting the essential contribution of the GD and PGS to the electrochemical performance of graphite in AGDIBs.

The effects of the morphology of graphite were comprehensively studied in Ref. [95], where it was shown that the shape of the graphite also contributes significantly to the capacity and voltage profiles of the graphite. Comparison of graphite particles with flake and potato-shaped morphologies revealed that the potato particles had significantly lower capacity associated with the intercalation of large $AlCl_4^-$, as opposed to the case of smaller Li^+ ions. Specifically, potato-shaped graphite demonstrated a much lower capacity of 65 mA h g^{-1} in comparison with large graphite flakes (0.2–1 mm in lateral size), which showed a remarkably high capacity of 95 mA h g^{-1}. As shown by Kravchyk et al. [95], flake-shaped graphite with accessible edges are essential for the intercalation of large $AlCl_4^-$ ions.

4.2.1.1.2.3. Other factors contributing to the electrochemical performance of graphite in AGDIBs

Overall, aside from the contributions from the structure and morphology of the graphite particles, the voltage and capacities of graphite vary significantly upon many other factors such as the nature of the electrolyte, cycling protocol, and temperature. For example, as shown by Wang et al. [229], the acidity of an $AlCl_3$-EMIMCl ionic liquid has a significant impact on the voltage profiles of positive graphite electrodes, where the higher the acidity is, the lower the average voltage

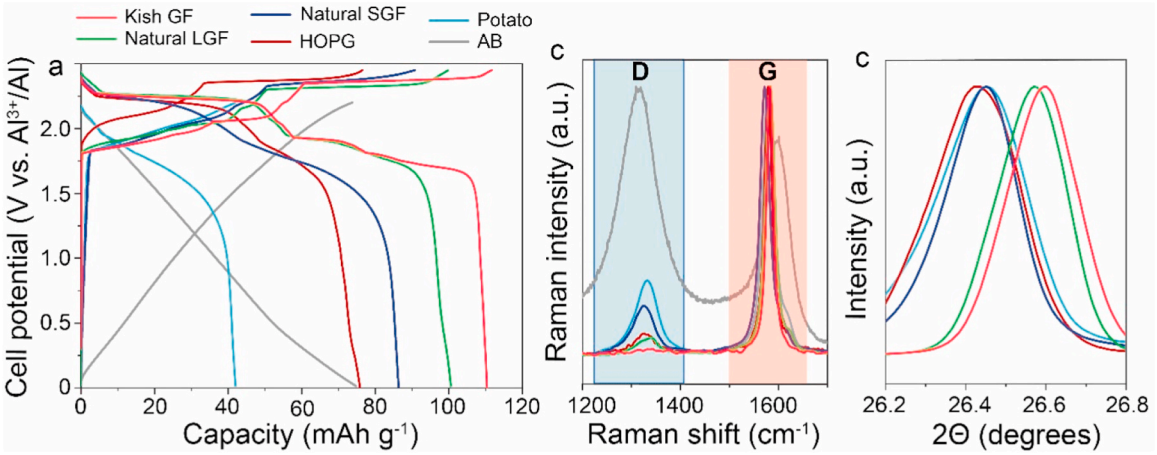

Fig. 9. (a) Galvanostatic voltage profiles of various carbonous materials [kish GF, kish graphite flakes (2 mm); Natural LGF, natural large graphite flakes (1 mm); Natural SGF, natural small graphite flakes (8 μm); HOPG, highly oriented pyrolytic graphite; Potato, potato-shaped particles from MTI company (30 μm); AB, acetylene black (26 μm)] measured at a current density of 50 mA g^{-1} using $AlCl_3$:EMIMCl ionic liquid ($r = 1.3$). Adapted from Refs. [95], ACS. (b) Raman spectroscopy and (c) X-ray diffraction measurements of various carbonous materials. Adapted from Ref. [98], ACS.

is. Interestingly, Wang et al. [229] assessed the Al^{3+}/Al redox potential in $AlCl_3$-EMIMCl chloroaluminate melts *vs.* the standard hydrogen electrode using a specially made cell composed of a Na-ion conducting solid-state electrolyte (β-alumina) and a metallic sodium reference electrode. It was determined that Al plating/striping takes place at −0.7 V *vs.* SHE (2.3 V *vs.* Li^+/Li). These findings allow assessment of the intercalation potential of $AlCl_4^-$ ions into graphite *vs.* Li^+/Li, which is a similar range as the intercalation voltages of other anions.

Other important factors that must be discussed are the charging protocol and temperature because of their significant influence on the charge storage capacity of graphite. Specifically, it has been shown that upon charging of graphite using the constant current–constant voltage (CCCV) protocol that includes constant charging steps in the range of 1.9–2.1 V (terminated at a current drop of 90%), significantly higher capacities can be obtained, up to 150 mA h g^{-1} [98]. Constant voltage steps of higher voltages of >2.1 V were rather destructive and initiated side reactions and resulted in low Coulombic efficiency. Constant voltage steps at low voltages of <1.9 V had minimal effects on the capacity of graphite. Besides the CCCV charging protocol, increased charge storage capacity for the graphite in AGDIBs can also be achieved at low temperatures of *ca.* −10 °C, as reported by Chun-Jern Pan et al. [179].

4.2.1.1.2.4. Volumetric changes and current collector issues in AGDIBs

According to the mechanism of AGDIBs, both the chloroaluminate electrolyte and graphite undergo substantial volumetric changes during charging and discharging. For instance, the volume of graphite particles can increase up to 134% upon the intercalation of $AlCl_4^-$ ions [161,260,278]. On the contrary, minor volume changes of up to 10% occur upon the intercalation of Li^+ into graphite [279]. Such substantial volumetric variations have a considerable impact on the overall volume change of cell-level AGDIBs. Concurrently, depending on the acidity of the chloroaluminate electrolytes, the volume of the electrolyte can change significantly during cycling. As an example, the volumetric change of an $AlCl_3$:EMIMCl electrolyte can be up to 30%, corresponding to complete depletion of $Al_2Cl_7^-$ and $AlCl_4^-$ ions from the electrolyte at the maximum acidity ($r = 2$). Assuming the expansion of the graphite and shrinkage of the electrolyte upon charging, the overall volume expansion of AGDIBs can be estimated to be in the range of 20–25% [280]. Consequently, a compelling solution to this issue should invoke an entirely new AGDIB design that is vastly different from the design that is currently used in conventional Li-ion batteries. It should be noted that future work on AGDIBs should also be focused on the other issue associated with this type of battery, one being the incompatibility of most metallic current collectors with the corrosive chloroaluminate ionic liquids. Contrary to the well-known LIB systems that use Al foil as the conventional current collector at the positive electrode, the development of the cathodic current collector for AGDIBs is still in progress. For instance, stainless steel and aluminum are oxidized at 1.5–2.5 V *vs.* SHE upon graphite charging [228,229]. Thus far, only tungsten, molybdenum, glassy carbon, TiN, and Cr_2N have successfully been employed in AGDIBs as current collectors [229]. Therefore, the quest for suitable current collectors continues. It has become apparent that there is a pressing need to identify current collectors made of compounds made from elements of high natural abundance and availability at low manufacturing costs.

4.2.1.2. Al-organic dual-ion battery (AODIB). Organic electrodes use a coordination reaction mechanism where the redox reaction is based on changes in the state of charge of the electroactive organic groups or moieties of organic cathodes [281]. Organic electrodes have already demonstrated reversible electrochemical performance with different multivalent cations [282,283], and have very recently also been employed in Al-batteries [147,149,151]. Moreover, organic electrode materials can be produced from organic feedstock with a low environmental footprint [284] and are extremely tunable. Improved capacity and voltage can be obtained by modifying the functional groups and the chemical structure of the electrode. Furthermore, the rate capability is generally very good for Li, Na, and also divalent ions such as Mg [282]. For Al-batteries, one of the first attempts using an organic cathode was reported by Hudak [285], who showed the electrochemical activity of polypyrrole with chloroaluminate anions. The study indicated that $AlCl_4^-$ was the electroactive species, with an electrochemical process similar to a dual-ion cell. The use of the anion as the active specie implies the need of a certain amount of electrolyte to sustain the electrochemical reaction, thus compromising the energy density of the system. An alternative storage mechanism has been proposed by Kim et al. for phenanthrenequinone-based macrocycles, which have a reversible capacity of 110 mA h g^{-1} and a cyclability of up to 5000 cycles. The group suggested that $AlCl_2^+$ was the electrochemically active ion, as indicated by the elemental composition ratio obtained by ex-situ EDX and TOF-SIMS. Similarly, Bitenc et al. [149] indicated that $AlCl_2^+$ was the electroactive species for an anthraquinone (AQ) based cathode. The use of $AlCl_2^+$ as the electroactive specie mitigates the amount of electrolyte needed to sustain the electrochemical reaction, improving the theoretical energy density attainable by the battery. Table 4reports a summary of the Al/organic electrode systems reported in the literature. Al/organic cathode cells are characterized by a capacity ranging between 90 and 150 mA h g^{-1}, operating at voltages ranging between 1.1 and 1.7 V.

Table 4
Summary of the sulfur cathodes used in Al-batteries.

Cathode composition	Delivered capacity	Average voltage	Capacity retention	Cell configuration	Ref.
Sulfur-carbon composite (S–C) prepared through a melt-diffusion on an activated carbon cloth	1300 mA h g^{-1} @ 50 mA g^{-1}	*0.6 V*	*76% after 22 cycles @ 50 mA g^{-1}*	*Al/EMIMCl: $AlCl_3$ 1:1.5/ S–C Loading AM 0.8-1.0 mg cm^{-2}*	[80]
S@CMK-3 Cathode prepared through a melt-diffusion	1500 mA h g^{-1} @ 251 mA g^{-1}	*0.6 V*	*40% after 20 cycles @ 251 mA g^{-1}*	*Al/BMPy*: $AlCl_3$ 1:1.3/ S@CMK-3 Loading AM n/a*	[172]
S@CNF paper	1250 mA h g^{-1} @ 83.75 mA g^{-1}	*0.8 V*	*50% after 10 cycles @ 83.75 mA g^{-1}*	*Al/EMIMCl: $AlCl_3$ 1:1.3/ S@CNF Loading AM 1 mg cm^{-2}*	[82]
S@CMK-3 Cathode prepared through a melt-diffusion	2000 mA h g^{-1} @ 100 A g^{-1}	*0.6 V*	*25% after 60 cycles @ 100 mA g^{-1}*	*Al/EMIMCl: $AlCl_3$ 1:1.5/ S@CMK-3 Loading AM 0.25 mg cm^{-2}*	[148]
S@ multi-walled carbon nanotubes (CNT) Cathode prepared through a melt-diffusion	2100 mA h g^{-1} @ 50 mA g^{-1}	*0.5 V*	*20% after 10 cycles @ 50 mA g^{-1}*	*Al/acetamide: $AlCl_3$ 1:1.5/ S@CNT Loading AM 0.2 mg cm^{-2}*	[86]
	500 mA h g^{-1} @ 50 A g^{-1}	*0.3 V*		*Al/acetamide: $AlCl_3$ 1:1.5/ S@CNT Loading AM 1.75 mg cm^{-2}*	
Self-protonated Polyaniline (PANI-H)	2300 mA h g^{-1} @ 50 mA g^{-1}	*0.5 V*	*7% after 10 cycles @ 50 mA g^{-1}*	*Al/urea:$AlCl_3$ 1:1.5/S@CNT Loading AM 0.2 mg cm^{-2}*	
	150 mA h g^{-1} @ 50 A g^{-1}	*0.3 V*		*Al/urea:$AlCl_3$ 1:1.5/S@CNT Loading AM 1.75 mg cm^{-2}*	
	1400 mA h g^{-1} @ 50 mA g^{-1}	*0.3 V*	*30% after 10 cycles @ 50 mA g^{-1}*	*Al/EMIMCl: $AlCl_3$ 1:1.5/ S@CNT Loading AM 0.2 mg cm^{-2}*	
	1000 mA h g^{-1} @ 50 A g^{-1}	*0.3 V*		*Al/EMIMCl: $AlCl_3$ 1:1.5/ S@CNT Loading AM 1.75 mg cm^{-2}*	

Overall, cells are characterized by long cycle lives and very good rate capability has been reported. However, the majority of reports have utilized electrodes with a relatively low active material loading (0.5–1.0 mg cm^{-2}). Evaluation of the electrode material loading on the performance is an important parameter that should be verified for practical applications. Additionally, the reaction mechanism involves the $AlCl_4^-$ ion or the $AlCl_2^+$ ion, thus, similar to AGDIBs, the electrolyte must be utilized to sustain the electrochemical process, which can negatively influence the overall cell energy density.

4.2.2. Rocking chair Al-battery cathode

4.2.2.1. Sulfur. Sulfur based cathodes have also been widely investigated due to their high theoretical energy density of 1340 Wh kg^{-1} from the conversion reaction between S and Al ($2Al + 3S = Al_2S_3$). Investigations of sulfur-based cathodes in chloroaluminate melts can be dated back to the 80s, when Marassi et al. [286–288] investigated sulfur in NaCl–$AlCl_3$ electrolyte melts and showed that the electrochemical reaction involves the formation of aluminum chloride species in the electrolyte media. A second recent attempt has been reported by Archer and co-workers [79] who evaluated an Al/$AlCl_3$-EMIMCl/S battery and showed that the system can deliver a capacity of 1500 mA h g^{-1}, with respect to the mass of the sulfur, and an average working voltage of approximately 1.1–1.2 V. However, the proposed configuration can be considered a primary battery since the complete solubilization of the sulfur species in the electrolyte made it impossible to recharge the battery. A reversible Al/S cell using chloroaluminate melts was reported by Gao et al. [80] in 2016, indicating that, in disagreement with Archer and co-workers [79], the sulfur and intermediate Al_xS_y species have limited solubility in the melt electrolyte. The Al/$AlCl_3$-EMIMCl/S cycling test showed good stability upon cycling (30 cycles) and an elevated discharge capacity (1000 mA h g^{-1} respect to the mass of sulfur). However, the system was characterized by increased polarization associated with the kinetically limited solid-state sulfur conversion reaction. Yang et al. [172] proposed the use of $Al_2Cl_6Br^-$ instead of Al_2Cl_7 to take advantage of the lower electronegativity (2.96) and larger covalent radius (120 p.m.) of Br with respect to the Cl (electronegativity 3.16 and covalent radius 102 p.m.), which was expected to result in a weaker bridge bond (Al–Br) and consequently a higher dissociation rate for the formation of Al_xS_y species. The reported results showed an improvement in the electrochemical process of Al–S batteries with enhanced charge/discharge kinetics by employing the Br-based electrolyte [172].

A detailed investigation of the reversibility of the Al/S system has been reported by Manthiram and co-workers [82]. Their study indicated that the electrochemical process involves the formation of a series of polysulfides and sulfide. UV–vis results showed that only high order polysulfides are soluble in the electrolyte. As seen in Fig. 10a, the peak at 330 nm, indicates the existence of a soluble species of S_6^{2-}. The results did not support the presence of S_4^{2-} or S_3^-, suggesting the low order polysulfides are insoluble in the EMIMCl:$AlCl_3$ electrolyte. The ex-situ measurements reported in Fig. 10e show that S_6^{2-} is also visible for the fully discharged and fully charged states, indicating that the species is not completely converted into the final discharge/charge product. Confirmation of the partial reversibility of the system was also confirmed by ex-situ XPS (Fig. 10f–k). Table 5 reports a summary of the Al/S cells reported in the literature. The overview shows elevated capacity values, indicating good overall utilization of the sulfur in the cathode. Indeed, in some cases the reported capacity exceeds the theoretical capacity of the sulfur, most likely due to the intercalation of $AlCl_4^-$ anions into the carbon substrates that are generally used for producing S–C composites. While the sulfur utilization is relatively good, all the reports show elevated polarization, indicating there is limited kinetics for the conversion reaction. Generally, a discharge voltage of 0.6 V is reported, while the theoretical voltage is expected to be 1.1 V. Additionally, the system is characterized by limited stability upon cycling, generally not exceeding a few tens of cycles. Moreover, all the reports use a relatively low sulfur loading in the cathode, usually not exceeding 1 mg cm^{-2}. The report of Lampkin et al. [86] showed the negative effects of high sulfur loading on the electrochemical performance. For high sulfur loading electrodes, both the discharge capacity and working voltage are substantially reduced for cells that use DES electrolytes. On the contrary, employing the EMIMCl:$AlCl_3$ electrolyte allows for adequate Al/S cell operation.

5. Conclusion and perspective

Critical assessment of the diverse types of reported Al-batteries reveals that more research is still required to bring this technology towards higher technology readiness levels (TRLs). Table 6 presents the EU Set plan for the 2030 key performance indicators (KPIs) for e-mobility and

Table 5
Summary of the organic cathodes used in Al-batteries.

Cathode composition	Delivered capacity	Average voltage	Capacity retention	Cell configuration	Ref.
Polythiophene (PT)	88 mA h g^{-1} @ 16 mA g^{-1}	*1.4 V*	*80% after 100 cycles* @ 16 mA g^{-1}	*Al/EMIMCl:$AlCl_3$ 1:1.5/PQ Loading AM 0.5 mg cm^{-2}*	[285]
Phenanthrenequinone (PQ)	90 mA h g^{-1} @ 2 A g^{-1}	*1.4 V*	*55% after 5000 cycles* @ 2 A g^{-1}	*Al/EMIMCl:$AlCl_3$ 1:1.5/PQ Loading AM 0.5 mg cm^{-2}*	[151]
Anthraquinone (AQ)	150 mA h g^{-1} @ 125 mA g^{-1}	*1.1 V*	*70% after 500 cycles* @ 125 mA g^{-1}	*Al/EMIMCl:$AlCl_3$ 1:1.5/AQ Loading AM 2–3 mg cm^{-2}*	[149]
Phenanthrenequinone (PQ)	100 mA h g^{-1} @ 1 A g^{-1}	*1.1 V*	*90% after 8000 cycles* @ 1 A g^{-1}	*Al/EMIMCl:$AlCl_3$ 1:1.5/PQ Loading AM 1 mg cm^{-2}*	[148]
Poly(nitropyrene-co-pyrene) (PNP)	100 mA h g^{-1} @ 200 mA g^{-1}	*1.7 V*	*80% after 1000 cycles* @ 200 mA g^{-1}	*Al/EMIMCl:$AlCl_3$ 1:1.3/PNP Loading AM 0.5 mg cm^{-2}*	[147]
Self-protonated Polyaniline (PANI-H)	120 mA h g^{-1} @ 6 A g^{-1}	*1.1 V*	*87.6% after 8000 cycles* @ 6 A g^{-1}	*Al/EMIMCl:$AlCl_3$ 1:1.5/PANI-H Loading AM 1.1 mg cm^{-2} (2 and 4 mg cm^{-2} also tested)*	[252]

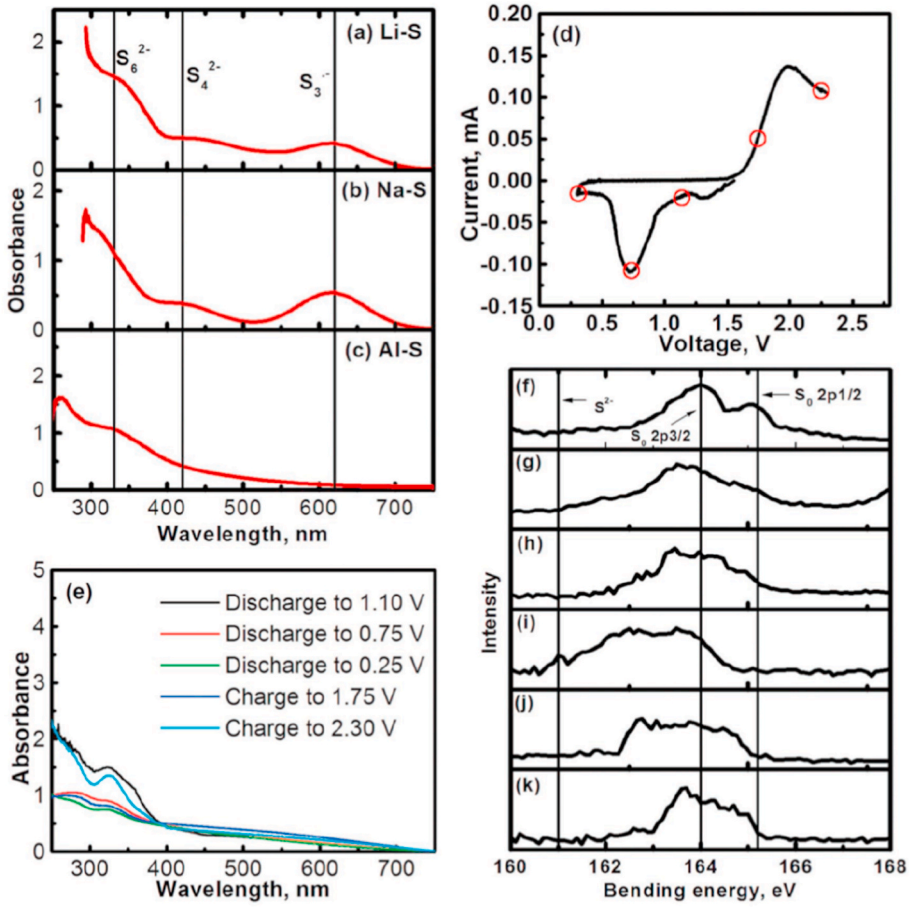

Fig. 10. UV–vis spectra of the sulfur cathodes discharged to a depth of 350 mA h g^{-1} in a) Li–S, b) Na–S, and c) Al–S cells. d) Specific potentials in the cyclic voltammetry profile of an Al ‖ SWCNT-GF ‖ S cell where samples for UV–vis and XPS analyses were collected. e) UV–vis spectra of the sulfur electrodes discharged or charged to different states. f–k) XPS S 2p spectra of the fresh sulfur electrode and those discharged or charged to different states: f) fresh sulfur electrode, g) discharged to 1.10 V, h) discharged to 0.75 V, i) discharged to 0.25 V, j) charged to 1.75 V, and k) charged to 2.30 V.

stationary storage [289] in comparison with the evaluated KPIs of commercial Li-ion battery (Panasonic NCR18650B) [291], a Na-ion battery prototype (TIAMAT) [292,293], and numerous Al-batteries, such as aqueous Al-ion, Al-air, and non-aqueous AGDI, AODI, and Al–S. The evaluated TRLs of most Al-systems range from 1 to 2, and only Al-air and AGDIB can be placed at a slightly higher TRLs of 3–4. Additionally, we can infer that the general performance of the various Al-batteries can hardly reach the requirements set in the EU set plan defined for Li-ion technology, and several relevant issues need to be solved. However, we must mention that a direct comparison of Li-ion technology with Al systems is not totally fair. Indeed, while lithium technology is a well-established system with 30 years of intensive research and development and billions of dollars of investments, aluminum systems are in a primordial stage with many open questions to be answered. Nonetheless, some remarks for the various cell configurations proposed so far can be given:

- The development of aqueous Al-ion batteries is driven by the possibility of high rate capability, intrinsic safety, low toxicity, and potentially low-cost storage devices. Aqueous electrolytes have the advantages of higher ionic conductivity (elevated power density) and easier handling, along with utilizing environmentally and chemically benign construction materials. The energy density, however, is limited due to the narrow electrochemical stability window of water compared to organic and ionic liquid electrolytes. For aqueous Al-ion cells, the high charge density of the Al^{+3} ion severely limits the choice of suitable cathode materials. For that reason, only a limited number of suitable materials have been

Table 6
Comparison of the energy densities of the most investigated Al-battery technologies in comparison with the EU Set plan for 2030. * Evaluation based on active materials only. † See Table S1 for details.

	Energy and power density	Cycle life	Cost	TRL in 2020	TRL in 2030	Reference
EU Set plan 2030 e-mobility Energy oriented	400 Wh kg^{-1} > 750 Wh l^{-1}	*2000 cycles at 80% DoD*	*< 100 €/kWh*	–	*TRL9*	[289]
EU Set plan 2030 e-mobility Power oriented	> 700 W kg^{-1} > 1500 W L^{-1}	*> 15000 cycles*	*< 100€/kWh*	–	*TRL9*	[289]
EU Set plan 2030 stationary storage	> 750 Wh l^{-1}	*10000 cycles, 20 years*	*0.05 €/kWh/cycle*	–	*TRL9*	[289]
Li-cell Panasonic NCR18650B	243 Wh kg^{-1} 676 Wh l^{-1}	*> 500 cycles*		*TRL9*		[291]
TIAMAT Na-ion battery	120 Wh kg^{-1}	*> 4000 cycles*		*TRL7*		[292,293]
Al-air	900 Wh kg^{-1}* 700 Wh l^{-1}*	*Not rechargeable*	*250 €/kWh*	*TRL 3-4*	—	[60]
Aqueous Al-batteries	30 kW kg^{-1}* 10 Wh kg^{-1}*	*> 7000 cycles*	—	*TRL 1-2*	—	[19]
AGDIB	65 Wh kg^{-1}* 92 Wh l^{-1}*	*> 10000 cycles*	*0.03 €/kWh/cycle*†	*TRL 4*	—	[20,105]
Al/S	400 Wh kg^{-1}*	*20 cycles*	—	*TRL 1-2*	—	[80,86]
Al/organic electrode	100 Wh kg^{-1}*	*> 5000 cycles*	—	*TRL 1-2*	—	[147,252]
T-Al/MnO_2	400 Wh kg^{-1}*	*20 cycles*	—	*TRL 1-2*	—	[28]

identified, such as TiO_2, V_2O_5, and Prussian blue. Moreover, most of the electrochemical tests are performed in three-electrode configurations using activated carbon or platinum as the counter electrode and an excess of electrolyte. Demonstrations of aqueous Al-ion batteries using full cell configurations with charge-storage balanced positive and negative electrodes are still relatively few. Many promises arrive from the possibility of using an Al stripping deposition process in aqueous electrolytes, upon surface treatment of the Al metal [28].

- The commercialization of Al-air batteries is limited by the severe corrosion of aluminum alloys in alkaline electrolytes. Additionally, the poor solubility of the $Al(OH)_4^-$ leads to clogging of the cathode [59]. Additionally, Al-air cells are non-rechargeable batteries, which is a clear disadvantage. However, a closed value chain where Al_2O_3 is formed as the discharged product in the cell and then regenerated to Al-metal via electrodeposition of molten salts is a possible solution. However, this production method is energy consuming and generates significant quantities of CO_2. The production of 1 kg of Al from Al_2O_3 requires 56 MJ of electricity and generates 15 kg of CO_2. The use of more sustainable production methods, such as the ELYSIS process developed by Alcoa [290], is fundamental to bring this technology to practical application.
- Chloroaluminate melts are the most used electrolyte for secondary Al-batteries thanks to the capability of efficient Al stripping/deposition processes in this electrolyte. However, several drawbacks are associated with this chemistry. The elevated corrosivity and reactivity of chloroaluminate melts are important aspects to consider in performing electrochemical tests and for the future development of such systems. Before performing any electrochemical characterization, the chemical and electrochemical stability of the test cell should be verified. It is always recommended to report electrochemical reference tests for the stability of the cell used. Additionally, the chemical stability of the investigated cathode material in the chloroaluminate melt should be verified. For the future development of this technology, the stability of the low-cost cell components (current collector, cell casing, separator, sealing glues) in chloroaluminate electrolytes needs to be investigated [229]. Alternatively, the development of electrolyte compositions with reduced reactivity that maintain the capability for efficient Al stripping/deposition processes can contribute to a breakthrough for this technology. The use of chlorine-free systems, as proposed by Johansson's group [194], can also be a valuable route to follow.
- AGDIBs are the most mature secondary Al-battery technology that has high potential for stationary energy storage applications because of their low cost and relatively high energy densities of up to ≈70 Wh kg^{-1}. The cost of the cell, evaluated on the 1 Ah cell prototype developed at Albufera is about 0.153€ (See Table S1). Similar to all dual-ion electrochemical systems, AGDIB electrolytes (anolytes) are an electrochemically active and rate-limiting battery component. The capacity of the anolyte is defined by its acidity (r). For instance, the theoretical gravimetric charge storage capacities of an $AlCl_3$: EMIMCl ionic liquid is equal to 48 mA h g^{-1} and 19 mA h g^{-1} for $r = 2$ and $r = 1.3$, respectively [105]. It should be stressed, however, that most literature reports on AGDIBs utilize anolytes with quite low acidities of $r = 1.3$. This causes severe limitations on the energy density of AGDIBs, which cannot exceed 30 Wh kg^{-1}, no matter how high the capacity of the graphite cathode is. Further research on AGDIBs should be focused on the most acidic anolyte formulations and finding practical amounts of the anolyte that are needed for the operation of AGDIBs.
- AODIBs are considered a promising system; thanks to the environmental friendliness of organic electrode materials and their overall suitable performance in terms of delivered capacity and operating voltage. However, similarly to AGDIBs, the involvement of the electrolyte in the electrochemical charge storage process has negative impact on the energy density of AODIBs.
- Al–S batteries are an extremely interesting technology that has elevated theoretical energy density values. However, only lab-scale cells with a limited number of cycles and relatively low electroactive material loading have been reported. A detailed investigation of the reaction mechanism is needed to identify the critical parameters to modify in order to obtain improved performance. The elevated overpotential of Al–S batteries, due to the slow kinetics of the conversion reaction, is one of the main problems to solve. Additionally, a clear identification of the reason behind capacity degradation is fundamental to achieve long cycle life batteries.

Overall, the overview of Al-batteries shows that there is a considerable gap between Al-battery systems and Li-ion technology. The evaluation suggested that for Al-batteries, it will be extremely challenging to reach KPIs close to Li-ion systems. However, Al-batteries can offer several advantages over the more mature Li-ion technology, and after proper maturation, can find their application niche. The most suitable application for Al-battery technology will be stationary storage, due to the expected low cost and high sustainability of Al-based systems. Material discovery platforms using high throughput systems combined with artificial intelligence computing can be fundamental to advance research on that topic. A completely new approach is required to achieve new electrolyte chemistries in order to find an alternative to chloroaluminate compositions or a solution to the elevated reactivity of chloroaluminates.

CRediT authorship contribution statement

Giuseppe Antonio Elia: Writing - original draft, Writing - review & editing, Supervision. **Kostiantyn V. Kravchyk:** Writing - original draft, Writing - review & editing. **Maksym V. Kovalenko:** Writing - original draft, Writing - review & editing. **Joaquín Chacón:** Writing - original draft, Writing - review & editing. **Alex Holland:** Writing - original draft, Writing - review & editing. **Richard G.A. Wills:** Writing - original draft, Writing - review & editing.

Declaration of competing interest

The authors declare that they have no known competing financial interests or personal relationships that could have appeared to influence the work reported in this paper

Acknowledgements

Financial support from the Helmholtz Association is also acknowledged. This research is part of the activities of SCCER HaE, which is financially supported by Innosuisse – Swiss Innovation Agency.

Appendix A. Supplementary data

Supplementary data to this article can be found online at https://doi.org/10.1016/j.jpowsour.2020.228870.

References

[1] EC Energy Roadmap 2050, Luxembourg: Publications Office of the European Union, 2012, https://doi.org/10.2833/10759.
[2] T.M. Gür, Review of electrical energy storage technologies, materials and systems: challenges and prospects for large-scale grid storage, Energy Environ. Sci. 11 (2018) 2696–2767, https://doi.org/10.1039/C8EE01419A.
[3] G. de Oliveira e Silva, P. Hendrick, Photovoltaic self-sufficiency of Belgian households using lithium-ion batteries, and its impact on the grid, Appl. Energy 195 (2017) 786–799, https://doi.org/10.1016/j.apenergy.2017.03.112.
[4] D. Larcher, J.-M. Tarascon, Towards greener and more sustainable batteries for electrical energy storage, Nat. Chem. 7 (2015) 19–29, https://doi.org/10.1038/nchem.2085.
[5] N. Yabuuchi, K. Kubota, M. Dahbi, S. Komaba, Research development on sodium-ion batteries, Chem. Rev. 114 (2014) 11636–11682, https://doi.org/10.1021/cr500192f.
[6] X. Ren, Y. Wu, A low-overpotential potassium–oxygen battery based on potassium superoxide, J. Am. Chem. Soc. 135 (2013) 2923–2926, https://doi.org/10.1021/ja312059q.
[7] A. Ponrouch, C. Frontera, F. Bardé, M.R. Palacín, Towards a calcium-based rechargeable battery, Nat. Mater. 15 (2015) 169–172, https://doi.org/10.1038/nmat4462.
[8] D. Aurbach, Z. Lu, A. Schechter, Y. Gofer, H. Gizbar, R. Turgeman, Y. Cohen, M. Moshkovich, E. Levi, Prototype systems for rechargeable magnesium batteries, Nature 407 (2000) 724–727, https://doi.org/10.1038/35037553.
[9] G.A. Elia, K. Marquardt, K. Hoeppner, S. Fantini, R. Lin, E. Knipping, W. Peters, J.-F. Drillet, S. Passerini, R. Hahn, An overview and future perspectives of aluminum batteries, Adv. Mater. 28 (2016), https://doi.org/10.1002/adma.201601357.
[10] G.A. Elia, I. Hasa, G. Greco, T. Diemant, K. Marquardt, K. Hoeppner, R.J. Behm, A. Hoell, S. Passerini, R. Hahn, Insights into the reversibility of aluminum graphite batteries, J. Mater. Chem. A. 5 (2017) 9682–9690, https://doi.org/10.1039/C7TA01018D.
[11] U.S. Geological Survey, G.S. Circular, Mineral commodities summaries. https://doi.org/10.3133/70140094, 2015.
[12] M. Fleischer, Recent estimates of the abundances of the elements in this earth's crust, Geol. Surv. Circular 285 (1953).
[13] M.-C. Lin, M. Gong, B. Lu, Y. Wu, D.-Y. Wang, M. Guan, M. Angell, C. Chen, J. Yang, B.-J. Hwang, H. Dai, An ultrafast rechargeable aluminium-ion battery, Nature 520 (2015) 324–328, https://doi.org/10.1038/nature14340.
[14] H. Zhang, X. Liu, H. Li, I. Hasa, S. Passerini, Challenges and strategies for high-energy aqueous electrolyte rechargeable batteries, Angew. Chem. Int. Ed. 59 (2020) 2–21, https://doi.org/10.1002/anie.202004433.
[15] W. Li, J.R. Dahn, D.S. Wainwright, Rechargeable lithium batteries with aqueous electrolytes, Science 264 (1994) 1115–1118, https://doi.org/10.1126/science.264.5162.1115, 80.
[16] H. Kim, J. Hong, K.-Y. Park, H. Kim, S.-W. Kim, K. Kang, Aqueous rechargeable Li and Na ion batteries, Chem. Rev. 114 (2014) 11788–11827, https://doi.org/10.1021/cr500232y.
[17] Y. Wang, Z. Feng, D. Laul, W. Zhu, M. Provencher, M.L. Trudeau, A. Guerfi, K. Zaghib, Ultra-low cost and highly stable hydrated FePO 4 anodes for aqueous sodium-ion battery, J. Power Sources 374 (2018) 211–216, https://doi.org/10.1016/j.jpowsour.2017.10.088.
[18] L.-P. Wang, P.-F. Wang, T.-S. Wang, Y.-X. Yin, Y.-G. Guo, C.-R. Wang, Prussian blue nanocubes as cathode materials for aqueous Na-Zn hybrid batteries, J. Power Sources 355 (2017) 18–22, https://doi.org/10.1016/j.jpowsour.2017.04.049.
[19] A. Holland, R.D. Mckerracher, A. Cruden, R.G.A. Wills, An aluminium battery operating with an aqueous electrolyte, J. Appl. Electrochem. 48 (2018) 243–250, https://doi.org/10.1007/s10800-018-1154-x.
[20] L. Ellingsen, A. Holland, J.-F. Drillet, W. Peters, M. Eckert, C. Concepcion, O. Ruiz, J.-F. Colin, E. Knipping, Q. Pan, R. Wills, G. Majeau-Bettez, Environmental screening of electrode materials for a rechargeable aluminum battery with an AlCl3/EMIMCl electrolyte, Materials 11 (2018) 936, https://doi.org/10.3390/ma11060936.
[21] C. Helbig, A.M. Bradshaw, L. Wietschel, A. Thorenz, A. Tuma, Supply risks associated with lithium-ion battery materials, J. Clean. Prod. 172 (2018) 274–286, https://doi.org/10.1016/j.jclepro.2017.10.122.
[22] D. Kushnir, B.A. Sandén, The time dimension and lithium resource constraints for electric vehicles, Resour. Pol. 37 (2012) 93–103, https://doi.org/10.1016/j.resourpol.2011.11.003.
[23] A. Burke, Ultracapacitor technologies and application in hybrid and electric vehicles, Int. J. Energy Res. 34 (2010) 133–151, https://doi.org/10.1002/er.1654.
[24] K.W. Nam, S. Kim, S. Lee, M. Salama, I. Shterenberg, Y. Gofer, J.-S. Kim, E. Yang, C.S. Park, J.-S. Kim, S.-S. Lee, W.-S. Chang, S.-G. Doo, Y.N. Jo, Y. Jung, D. Aurbach, J.W. Choi, The high performance of crystal water containing manganese birnessite cathodes for magnesium batteries, Nano Lett. 15 (2015) 4071–4079, https://doi.org/10.1021/acs.nanolett.5b01109.
[25] A. Manthiram, An outlook on lithium ion battery technology, ACS Cent. Sci. 3 (2017) 1063–1069, https://doi.org/10.1021/acscentsci.7b00288.
[26] F. Jiang, P. Peng, Elucidating the performance limitations of lithium-ion batteries due to species and charge transport through five characteristic parameters, Sci. Rep. 6 (2016) 32639, https://doi.org/10.1038/srep32639.
[27] X. Gu, J. Liu, J. Yang, H. Xiang, X. Gong, Y. Xia, First-Principles study of H + intercalation in layer-structured LiCoO 2, J. Phys. Chem. C 115 (2011) 12672–12676, https://doi.org/10.1021/jp202846p.
[28] Q. Zhao, M.J. Zachman, W.I. Al Sadat, J. Zheng, L.F. Kourkoutis, L. Archer, Solid electrolyte interphases for high-energy aqueous aluminum electrochemical cells, Sci. Adv. 4 (2018), https://doi.org/10.1126/sciadv.aau8131 eaau8131.
[29] S. He, J. Wang, X. Zhang, J. Chen, Z. Wang, T. Yang, Z. Liu, Y. Liang, B. Wang, S. Liu, L. Zhang, J.J. Huang, J.J. Huang, L.A. O'Dell, H. Yu, A high-energy aqueous aluminum-manganese battery, Adv. Funct. Mater. 29 (2019) 1–9, https://doi.org/10.1002/adfm.201905228.
[30] C. Wu, S. Gu, Q. Zhang, Y. Bai, M. Li, Y.Y. Yuan, H. Wang, X. Liu, Y.Y. Yuan, N. Zhu, F. Wu, H. Li, L. Gu, J. Lu, Electrochemically activated spinel manganese oxide for rechargeable aqueous aluminum battery, Nat. Commun. 10 (2019) 73, https://doi.org/10.1038/s41467-018-07980-7.
[31] C. Jiang, M. Wei, Z. Qi, T. Kudo, I. Honma, H. Zhou, Particle size dependence of the lithium storage capability and high rate performance of nanocrystalline anatase TiO2 electrode, J. Power Sources 166 (2007) 239–243, https://doi.org/10.1016/j.jpowsour.2007.01.004.
[32] Y. Xu, E. Memarzadeh Lotfabad, H. Wang, B. Farbod, Z. Xu, A. Kohandehghan, D. Mitlin, Nanocrystalline anatase TiO2: a new anode material for rechargeable sodium ion batteries, Chem. Commun. 49 (2013) 8973, https://doi.org/10.1039/c3cc45254a.
[33] N.T. Nguyen, S. Ozkan, I. Hwang, X. Zhou, P. Schmuki, Spaced TiO 2 nanotube arrays allow for a high performance hierarchical supercapacitor structure, J. Mater. Chem. A. 5 (2017) 1895–1901, https://doi.org/10.1039/C6TA10179H.
[34] X. Lu, G. Wang, T. Zhai, M. Yu, J. Gan, Y. Tong, Y. Li, Hydrogenated TiO 2 nanotube Arrays for supercapacitors, Nano Lett. 12 (2012) 1690–1696, https://doi.org/10.1021/nl300173j.
[35] Y. Zhang, Y. Zhao, S. Cao, Z. Yin, L. Cheng, L. Wu, Design and synthesis of hierarchical SiO 2 @C/TiO 2 hollow spheres for high-performance supercapacitors, ACS Appl. Mater. Interfaces 9 (2017) 29982–29991, https://doi.org/10.1021/acsami.7b08776.
[36] S. Liu, J.J. Hu, N.F. Yan, G.L. Pan, G.R. Li, X.P. Gao, Aluminum storage behavior of anatase TiO2 nanotube arrays in aqueous solution for aluminum ion batteries, Energy Environ. Sci. 5 (2012) 9743–9746, https://doi.org/10.1039/c2ee22987k.
[37] Y. Liu, S. Sang, Q. Wu, Z. Lu, K. Liu, H. Liu, The electrochemical behavior of Cl-assisted Al3+ insertion into titanium dioxide nanotube arrays in aqueous solution for aluminum ion batteries, Electrochim. Acta 143 (2014) 340–346, https://doi.org/10.1016/j.electacta.2014.08.016.
[38] I. Shterenberg, M. Salama, H.D. Yoo, Y. Gofer, J.-B. Park, Y.-K. Sun, D. Aurbach, Evaluation of (CF 3 SO 2) 2 N − (TFSI) based electrolyte solutions for Mg batteries, J. Electrochem. Soc. 162 (2015) A7118–A7128, https://doi.org/10.1149/2.0161513jes.
[39] M. Kazazi, P. Abdollahi, M. Mirzaei-Moghadam, High surface area TiO2 nanospheres as a high-rate anode material for aqueous aluminium-ion batteries, Solid State Ionics 300 (2017) 32–37, https://doi.org/10.1016/j.ssi.2016.11.028.
[40] H. Lahan, R. Boruah, A. Hazarika, S.K. Das, Anatase TiO 2 as an anode material for rechargeable aqueous aluminum-ion batteries: remarkable graphene induced aluminum ion storage phenomenon, J. Phys. Chem. C 121 (2017) 26241–26249, https://doi.org/10.1021/acs.jpcc.7b09494.
[41] Z. Li, S. Ganapathy, Y. Xu, Z. Zhou, M. Sarilar, M. Wagemaker, Mechanistic insight into the electrochemical performance of Zn/VO2 batteries with an

aqueous ZnSO4 electrolyte, Adv. Energy Mater. 9 (2019) 1–10, https://doi.org/10.1002/aenm.201900237.
[42] M. Yan, P. He, Y. Chen, S. Wang, Q. Wei, K. Zhao, X. Xu, Q. An, Y. Shuang, Y. Shao, K.T. Mueller, L. Mai, J. Liu, J. Yang, Water-lubricated intercalation in V2O5·nH2O for high-capacity and high-rate aqueous rechargeable zinc batteries, Adv. Mater. 30 (2018), https://doi.org/10.1002/adma.201703725.
[43] F. Wan, L. Zhang, X. Dai, X. Wang, Z. Niu, J. Chen, Aqueous rechargeable zinc/sodium vanadate batteries with enhanced performance from simultaneous insertion of dual carriers, Nat. Commun. 9 (2018) 1–11, https://doi.org/10.1038/s41467-018-04060-8.
[44] F. Ming, H. Liang, Y. Lei, S. Kandambeth, M. Eddaoudi, H.N. Alshareef, Layered Mg xV2O5· nH2O as cathode material for high-performance aqueous zinc ion batteries, ACS Energy Lett 3 (2018) 2602–2609, https://doi.org/10.1021/acsenergylett.8b01423.
[45] M. Amati, C. Lenardi, R.G. Agostino, T. Caruso, C. Ducati, S. La Rosa, G. Bongiorno, V. Cassina, P. Podestà, L. Ravagnan, P. Piseri, P. Milani, Electrical conductivity of cluster-assembled carbon/titania nanocomposite films irradiated by highly focused vacuum ultraviolet photon beams, J. Appl. Phys. 101 (2007), 064314, https://doi.org/10.1063/1.2437658.
[46] W. Zhong, S. Sang, Y. Liu, Q. Wu, K. Liu, H. Liu, Electrochemically conductive treatment of TiO2 nanotube arrays in AlCl3 aqueous solution for supercapacitors, J. Power Sources 294 (2015) 216–222, https://doi.org/10.1016/j.jpowsour.2015.06.052.
[47] J.-Y. Luo, W.-J. Cui, P. He, Y.-Y. Xia, Raising the cycling stability of aqueous lithium-ion batteries by eliminating oxygen in the electrolyte, Nat. Chem. 2 (2010) 760–765, https://doi.org/10.1038/nchem.763.
[48] J. Qian, C. Wu, Y. Cao, Z. Ma, Y. Huang, X. Ai, H. Yang, Prussian blue cathode materials for sodium-ion batteries and other ion batteries, Adv. Energy Mater. 8 (2018) 1702619, https://doi.org/10.1002/aenm.201702619.
[49] S. Liu, G.L. Pan, G.R. Li, X.P. Gao, Copper hexacyanoferrate nanoparticles as cathode material for aqueous Al-ion batteries, J. Mater. Chem. A. 3 (2015) 959–962, https://doi.org/10.1039/c4ta04644g.
[50] X. Xu, F. Xiong, J. Meng, Q. An, L. Mai, Multi-electron reactions of vanadium-based nanomaterials for high-capacity lithium batteries: challenges and opportunities, Mater. Today Nano. (2020), https://doi.org/10.1016/j.mtnano.2020.100073.
[51] M. Song, H. Tan, D. Chao, H.J. Fan, Recent advances in Zn-ion batteries, Adv. Funct. Mater. 28 (2018) 1–27, https://doi.org/10.1002/adfm.201802564.
[52] J.R. González, F. Nacimiento, M. Cabello, R. Alcántara, P. Lavela, J.L. Tirado, Reversible intercalation of aluminium into vanadium pentoxide xerogel for aqueous rechargeable batteries, RSC Adv. 6 (2016) 62157–62164, https://doi.org/10.1039/c6ra11030d.
[53] A.W. Holland, A. Cruden, A. Zerey, A. Hector, R.G.A. Wills, Electrochemical study of TiO2 in aqueous AlCl3 electrolyte via vacuum impregnation for superior high-rate electrode performance, BMC Energy 1 (2019) 10, https://doi.org/10.1186/s42500-019-0010-9.
[54] H.-C. Tao, X.-L. Yang, L.-L. Zhang, S.-B. Ni, Double-walled core-shell structured Si@SiO2@C nanocomposite as anode for lithium-ion batteries, Ionics 20 (2014) 1547–1552, https://doi.org/10.1007/s11581-014-1138-8.
[55] T.B. Reddy, Linden's Handbook of Batteries, fourth ed., fourth ed., McGraw-Hill Education, New York, n.d.
[56] D.R. Egan, C. Ponce de León, R.J.K. Wood, R.L. Jones, K.R. Stokes, F.C. Walsh, Developments in electrode materials and electrolytes for aluminium–air batteries, J. Power Sources 236 (2013) 293–310, https://doi.org/10.1016/j.jpowsour.2013.01.141.
[57] A.R. Despic, The use of aluminium in energy conversion and storage, in: First Eur. East-West Work. Energy Convers. Storage, 1990.
[58] http://www.phinergy.com/, 2020. (Accessed 3 September 2020).
[59] J. Ryu, M. Park, J. Cho, Advanced technologies for high-energy aluminum–air batteries, Adv. Mater. 31 (2019) 1804784, https://doi.org/10.1002/adma.201804784.
[60] B.J. Hopkins, Y. Shao-Horn, D.P. Hart, Suppressing corrosion in primary aluminum–air batteries via oil displacement, Science 362 (80) (2018) 658–661, https://doi.org/10.1126/science.aat9149.
[61] E.I.I. Shkolnikov, A.Z.Z. Zhuk, M.S.S. Vlaskin, Aluminum as energy carrier: feasibility analysis and current technologies overview, Renew. Sustain. Energy Rev. 15 (2011) 4611–4623, https://doi.org/10.1016/j.rser.2011.07.091.
[62] C. Vargel, Introduction to the corrosion of aluminium, in: Corros. Alum, Elsevier, 2004, pp. 81–109, https://doi.org/10.1016/B978-008044495-6/50011-2.
[63] M.D. Dyar, M.E. Gunter, D. Tasa, Mineralogy and Optical Mineralogy, 2008.
[64] G. Djukanovic, Aluminum: world market prospects for troubled times, JOM (J. Occup. Med.) 61 (2009) 63–66, https://doi.org/10.1007/s11837-009-0030-x.
[65] W.R. Hale, The global light metals sector outlook: a primary aluminum perspective, JOM (J. Occup. Med.) 52 (2000) 26.
[66] Pittsburgh, Alcoa 2009 Annual Report and Form 10-K, 2009.
[67] X. Huang, Y. Liu, C. Liu, J. Zhang, O. Noonan, C. Yu, Rechargeable aluminum-selenium batteries with high capacity, Chem. Sci. 9 (2018) 5178–5182, https://doi.org/10.1039/c8sc01054d.
[68] X. Xiao, M. Wang, J. Tu, Y. Luo, S. Jiao, Metal-organic framework-derived Co3O4@MWCNTs polyhedron as cathode material for a high-performance aluminum-ion battery, ACS Sustain. Chem. Eng. 7 (2019) 16200–16208, https://doi.org/10.1021/acssuschemeng.9b03159.
[69] J. Jiang, H. Li, T. Fu, B.J. Hwang, X. Li, J. Zhao, One-Dimensional Cu2-xSe nanorods as the cathode material for high-performance aluminum-ion battery, ACS Appl. Mater. Interfaces 10 (2018) 17942–17949, https://doi.org/10.1021/acsami.8b03259.
[70] Z. Li, J. Liu, X. Huo, J. Li, F. Kang, Novel one-dimensional hollow carbon nanotubes/selenium composite for high-performance Al-Se batteries, ACS Appl. Mater. Interfaces 11 (2019) 45709–45716, https://doi.org/10.1021/acsami.9b16597.
[71] X. Zhang, S. Jiao, J. Tu, W.L. Song, X. Xiao, S. Li, M. Wang, H. Lei, D. Tian, H. Chen, D. Fang, Rechargeable ultrahigh-capacity tellurium-aluminum batteries, Energy Environ. Sci. 12 (2019) 1918–1927, https://doi.org/10.1039/c9ee00862d.
[72] H. Lu, Y. Wan, T. Wang, R. Jin, P. Ding, R. Wang, Y. Wang, C. Teng, L. Li, X. Wang, D. Zhou, G. Xue, A high performance SnO2/C nanocomposite cathode for aluminum-ion batteries, J. Mater. Chem. A. 7 (2019) 7213–7220, https://doi.org/10.1039/c8ta11132d.
[73] A.P. Vijaya Kumar Saroja, A. Arjunan, K. Muthusamy, V. Balasubramanian, R. Sundara, Chemically bonded amorphous red phosphorous with disordered carbon nanosheet as high voltage cathode for rechargeable aluminium ion battery, J. Alloys Compd. 830 (2020) 154693, https://doi.org/10.1016/j.jallcom.2020.154693.
[74] J. Tu, M. Wang, Y. Luo, S. Jiao, Coral-like TeO2 microwires for rechargeable aluminum batteries, ACS Sustain. Chem. Eng. 8 (2020) 2416–2422, https://doi.org/10.1021/acssuschemeng.9b06193.
[75] Z. Yu, S. Jiao, J. Tu, Y. Luo, W.L. Song, H. Jiao, M. Wang, H. Chen, D. Fang, Rechargeable nickel telluride/aluminum batteries with high capacity and enhanced cycling performance, ACS Appl. Mater. Interfaces 14 (2020) 3469–3476, https://doi.org/10.1021/acsnano.9b09550.
[76] J. Wu, D. Wu, M. Zhao, Z. Wen, J. Jiang, J. Zeng, J. Zhao, Rod-shaped Cu1.81Te as a novel cathode material for aluminum-ion batteries, Dalton Trans. 49 (2020) 729–736, https://doi.org/10.1039/c9dt04157e.
[77] S. Choi, H. Go, G. Lee, Y. Tak, Electrochemical properties of an aluminum anode in an ionic liquid electrolyte for rechargeable aluminum-ion batteries, Phys. Chem. Chem. Phys. 19 (2017) 8653–8656, https://doi.org/10.1039/c6cp08776k.
[78] S. Lu, M. Wang, F. Guo, J. Tu, A. Lv, Y. Chen, S. Jiao, Self-supporting and high-loading hierarchically porous Co-P cathode for advanced Al-ion battery, Chem. Eng. J. 389 (2020) 124370, https://doi.org/10.1016/j.cej.2020.124370.
[79] G. Cohn, L. Ma, L.A. Archer, A novel non-aqueous aluminum sulfur battery, J. Power Sources 283 (2015) 416–422, https://doi.org/10.1016/j.jpowsour.2015.02.131.
[80] T. Gao, X. Li, X. Wang, J. Hu, F. Han, X. Fan, L. Suo, A.J. Pearse, S.B. Lee, G. W. Rubloff, K.J. Gaskell, M. Noked, C. Wang, A rechargeable Al/S battery with an ionic-liquid electrolyte, Angew. Chem. Int. Ed. 55 (2016) 9898–9901, https://doi.org/10.1002/anie.201603531.
[81] X. Yu, A. Manthiram, Ambient-temperature energy storage with polyvalent metal-sulfur chemistry, Small Methods 1 (2017) 1700217, https://doi.org/10.1002/smtd.201700217.
[82] X. Yu, A. Manthiram, Electrochemical energy storage with a reversible nonaqueous room-temperature aluminum–sulfur chemistry, Adv. Energy Mater. 7 (2017) 1–9, https://doi.org/10.1002/aenm.201700561.
[83] X. Yu, M.J. Boyer, G.S. Hwang, A. Manthiram, Room-temperature aluminum-sulfur batteries with a lithium-ion-mediated ionic liquid electrolyte, Inside Chem. 4 (2018) 586–598, https://doi.org/10.1016/j.chempr.2017.12.029.
[84] K. Zhang, T.H. Lee, J.H. Cha, R.S. Varma, J.W. Choi, H.W. Jang, M. Shokouhimehr, Two-dimensional boron nitride as a sulfur fixer for high performance rechargeable aluminum-sulfur batteries, Sci. Rep. 9 (2019) 1–10, https://doi.org/10.1038/s41598-019-50080-9.
[85] X. Zheng, R. Tang, Y. Zhang, L. Ma, X. Wang, Y. Dong, G. Kong, L. Wei, Design of a composite cathode and a graphene coated separator for a stable room-temperature aluminum-sulfur battery, Sustain. Energy Fuels 4 (2020) 1630–1641, https://doi.org/10.1039/c9se00762h.
[86] J. Lampkin, H. Li, L. Furness, R. Raccichini, N. Garcia-Araez, Novel electrolytes for aluminium-sulfur batteries: critical evaluation of electrode thickness effects and side reactions, ChemSusChem 13 (2020) 3514–3523, https://doi.org/10.1002/cssc.202000447.
[87] H. Jiao, J. Wang, J. Tu, H. Lei, S. Jiao, Aluminum-ion asymmetric supercapacitor incorporating carbon nanotubes and an ionic liquid electrolyte: Al/AlCl3-[EMIm]Cl/CNTs, Energy Technol. 4 (2016) 1112–1118, https://doi.org/10.1002/ente.201600125.
[88] Z.A. Zafar, S. Imtiaz, R. Li, J. Zhang, R. Razaq, Y. Xin, Q. Li, Z. Zhang, Y. Huang, A super-long life rechargeable aluminum battery, Solid State Ionics 320 (2018) 70–75, https://doi.org/10.1016/j.ssi.2018.02.037.
[89] K. Suto, A. Nakata, H. Murayama, T. Hirai, J. Yamaki, Z. Ogumi, Electrochemical properties of Al/vanadium chloride batteries with AlCl 3 -1-Ethyl-3-methylimidazolium chloride electrolyte, J. Electrochem. Soc. 163 (2016) A742–A747, https://doi.org/10.1149/2.0991605jes.
[90] H. Sun, W. Wang, Z. Yu, Y. Yuan, S. Wang, S. Jiao, A new aluminium-ion battery with high voltage, high safety and low cost, Chem. Commun. 51 (2015) 11892–11895, https://doi.org/10.1039/c5cc00542f.
[91] G.Y. Yang, L. Chen, P. Jiang, Z.Y. Guo, W. Wang, Z.P. Liu, Fabrication of tunable 3D graphene mesh network with enhanced electrical and thermal properties for high-rate aluminum-ion battery application, RSC Adv. 6 (2016) 47655–47660, https://doi.org/10.1039/c6ra06467a.
[92] X. Huang, Y. Liu, H. Zhang, J. Zhang, O. Noonan, C. Yu, Free-standing monolithic nanoporous graphene foam as a high performance aluminum-ion battery cathode, J. Mater. Chem. A. 5 (2017) 19416–19421, https://doi.org/10.1039/c7ta04477a.
[93] Y. Wu, M. Gong, M.C. Lin, C. Yuan, M. Angell, L. Huang, D.Y. Wang, X. Zhang, J. Yang, B.J. Hwang, H. Dai, 3D graphitic foams derived from chloroaluminate anion intercalation for ultrafast aluminum-ion battery, Adv. Mater. 28 (2016) 9218–9222, https://doi.org/10.1002/adma.201602958.

[94] S. Wang, S. Jiao, W.-L. Song, H.-S. Chen, J. Tu, D. Tian, H. Jiao, C. Fu, D.-N. Fang, A novel dual-graphite aluminum-ion battery, Energy Storage Mater 12 (2018) 119–127, https://doi.org/10.1016/j.ensm.2017.12.010.
[95] K.V. Kravchyk, S. Wang, L. Piveteau, M.V. Kovalenko, Efficient aluminum chloride–natural graphite battery, Chem. Mater. 29 (2017) 4484–4492, https://doi.org/10.1021/acs.chemmater.7b01060.
[96] S. Jiao, H. Lei, J. Tu, J. Zhu, J. Wang, X. Mao, An industrialized prototype of the rechargeable Al/AlCl3-[EMIm]Cl/graphite battery and recycling of the graphitic cathode into graphene, Carbon N. Y. 109 (2016) 276–281, https://doi.org/10.1016/j.carbon.2016.08.027.
[97] H. Chen, C. Chen, Y. Liu, X. Zhao, N. Ananth, B. Zheng, L. Peng, T. Huang, W. Gao, C. Gao, High-quality graphene microflower design for high-performance Li–S and Al-ion batteries, Adv. Energy Mater. 7 (2017) 1–9, https://doi.org/10.1002/aenm.201700051.
[98] S. Wang, K.V. Kravchyk, F. Krumeich, M.V. Kovalenko, Kish graphite flakes as a cathode material for an aluminum chloride–graphite battery, ACS Appl. Mater. Interfaces 9 (2017) 28478–28485, https://doi.org/10.1021/acsami.7b07499.
[99] H. Jiao, D. Tian, S. Li, C. Fu, S. Jiao, A rechargeable Al-Te battery, ACS Appl. Energy Mater. 1 (2018) 4924–4930, https://doi.org/10.1021/acsaem.8b00905.
[100] H. Chen, H. Xu, S. Wang, T. Huang, J. Xi, S. Cai, F. Guo, Z. Xu, W. Gao, C. Gao, Ultrafast all-climate aluminum-graphene battery with quarter-million cycle life, Sci. Adv. 3 (2017), https://doi.org/10.1126/sciadv.aao7233 eaao7233.
[101] C. Zhang, R. He, J. Zhang, Y. Hu, Z. Wang, X. Jin, Amorphous carbon-derived nanosheet-bricked porous graphite as high-performance cathode for aluminum-ion batteries, ACS Appl. Mater. Interfaces 10 (2018) 26510–26516, https://doi.org/10.1021/acsami.8b07590.
[102] J. Wei, W. Chen, D. Chen, K. Yang, An amorphous carbon-graphite composite cathode for long cycle life rechargeable aluminum ion batteries, J. Mater. Sci. Technol. 34 (2018) 983–989, https://doi.org/10.1016/j.jmst.2017.06.012.
[103] Q. Zhang, L. Wang, J. Wang, C. Xing, J. Ge, L. Fan, Z. Liu, X. Lu, M. Wu, X. Yu, H. Zhang, B. Lu, Low-temperature synthesis of edge-rich graphene paper for high-performance aluminum batteries, Energy Storage Mater 15 (2018) 361–367, https://doi.org/10.1016/j.ensm.2018.06.021.
[104] R.D. Mckerracher, A. Holland, A. Cruden, R.G.A. Wills, Comparison of carbon materials as cathodes for the aluminium-ion battery, Carbon N. Y. 144 (2019) 333–341, https://doi.org/10.1016/j.carbon.2018.12.021.
[105] K.V. Kravchyk, C. Seno, M.V. Kovalenko, Limitations of chloroaluminate ionic liquid anolytes for aluminum–graphite dual-ion batteries, ACS Energy Lett 5 (2020) 545–549, https://doi.org/10.1021/acsenergylett.9b02832.
[106] D.-Y. Wang, C.-Y. Wei, M.-C. Lin, C.-J. Pan, H.-L. Chou, H.-A. Chen, M. Gong, Y. Wu, C. Yuan, M. Angell, Y.-J. Hsieh, Y.-H. Chen, C.-Y. Wen, C.-W.C.-C. Chen, B.-J. Hwang, C.-W.C.-C. Chen, H. Dai, Advanced rechargeable aluminium ion battery with a high-quality natural graphite cathode, Nat. Commun. 8 (2017) 14283, https://doi.org/10.1038/ncomms14283.
[107] H. Chen, F. Guo, Y. Liu, T. Huang, B. Zheng, N. Ananth, Z. Xu, W. Gao, C. Gao, A defect-free principle for advanced graphene cathode of aluminum-ion battery, Adv. Mater. 29 (2017) 1605958, https://doi.org/10.1002/adma.201605958.
[108] Y. Chen, Z. Zhou, N. Li, S. Jiao, H. Chen, W.L. Song, D. Fang, Thick electrodes upon biomass-derivative carbon current collectors: high-areal capacity positive electrodes for aluminum-ion batteries, Electrochim. Acta 323 (2019) 1–9, https://doi.org/10.1016/j.electacta.2019.134805.
[109] J. Wang, J. Tu, H. Lei, H. Zhu, The effect of graphitization degree of carbonaceous material on the electrochemical performance for aluminum-ion batteries, RSC Adv. 9 (2019) 38990–38997, https://doi.org/10.1039/c9ra07234a.
[110] N.P. Stadie, S. Wang, K.V. Kravchyk, M.V. Kovalenko, Zeolite-templated carbon as an ordered microporous electrode for aluminum batteries, ACS Nano 11 (2017) 1911–1919, https://doi.org/10.1021/acsnano.6b07995.
[111] Z. Li, B. Niu, Y. Liu, J. Li, F. Kang, Prelithiation treatment of graphite as cathode material for rechargeable aluminum batteries, Electrochim. Acta 263 (2018) 68–75, https://doi.org/10.1016/j.electacta.2017.12.166.
[112] M.-C. Huang, C.-H. Yang, C.-C. Chiang, S.-C. Chiu, Y.-F. Chen, C.-Y. Lin, L.-Y. Wang, Y.-L. Li, C.-C. Yang, W.-S. Chang, Influence of high loading on the performance of natural graphite-based Al secondary batteries, Energies 11 (2018) 2760, https://doi.org/10.3390/en11102760.
[113] Y. Uemura, C.Y. Chen, Y. Hashimoto, T. Tsuda, H. Matsumoto, S. Kuwabata, Graphene nanoplatelet composite cathode for a chloroaluminate ionic liquid-based aluminum secondary battery, ACS Appl. Energy Mater. 1 (2018) 2269–2274, https://doi.org/10.1021/acsaem.8b00341.
[114] J.H. Xu, D.E. Turney, A.L. Jadhav, R.J. Messinger, Effects of graphite structure and ion transport on the electrochemical properties of rechargeable aluminum–graphite batteries, ACS Appl. Energy Mater. 2 (2019) 7799–7810, https://doi.org/10.1021/acsaem.9b01184.
[115] A.S. Childress, P. Parajuli, J. Zhu, R. Podila, A.M. Rao, A Raman spectroscopic study of graphene cathodes in high-performance aluminum ion batteries, Nanomater. Energy 39 (2017) 69–76, https://doi.org/10.1016/j.nanoen.2017.06.038.
[116] T.S. Lee, S.B. Patil, Y.T. Kao, J.Y. An, Y.C. Lee, Y.H. Lai, C.K. Chang, Y.S. Cheng, Y. C. Chuang, H.S. Sheu, C.H. Wu, C.C. Yang, R.H. Cheng, C.Y. Lee, P.Y. Peng, L. H. Lai, H.H. Lee, D.Y. Wang, Real-time observation of anion reaction in high performance Al ion batteries, ACS Appl. Mater. Interfaces 12 (2020) 2572–2580, https://doi.org/10.1021/acsami.9b20148.
[117] D. Novko, Q. Zhang, P. Kaghazchi, Nonadiabatic effects in Raman spectra of AlCl4–graphite based batteries, Phys. Rev. Appl. 12 (2019), https://doi.org/10.1103/PhysRevApplied.12.024016, 024016.
[118] C. Liu, Z. Liu, H. Niu, C. Wang, Z. Wang, B. Gao, J. Liu, M. Taylor, Preparation and in-situ Raman characterization of binder-free u-GF@CFC cathode for rechargeable aluminum-ion battery, Methods (Orlando) 6 (2019) 2374–2383, https://doi.org/10.1016/j.mex.2019.10.008.
[119] S. Zhang, X. Tan, Z. Meng, H. Tian, F. Xu, W.Q. Han, Naturally abundant high-performance rechargeable aluminum/iodine batteries based on conversion reaction chemistry, J. Mater. Chem. A. 6 (2018) 9984–9996, https://doi.org/10.1039/c8ta00675j.
[120] H. Tian, S. Zhang, Z. Meng, W. He, W.Q. Han, Rechargeable aluminum/iodine battery redox chemistry in ionic liquid electrolyte, ACS Energy Lett 2 (2017) 1170–1176, https://doi.org/10.1021/acsenergylett.7b00160.
[121] J. Liu, Z. Li, X. Huo, J. Li, Nanosphere-rod-like Co3O4 as high performance cathode material for aluminium ion batteries, J. Power Sources 422 (2019) 49–56, https://doi.org/10.1016/j.jpowsour.2019.03.029.
[122] S. Wang, Z. Yu, J. Tu, J. Wang, D. Tian, Y. Liu, S. Jiao, A novel aluminum-ion battery: Al/AlCl 3 -[EMIm]Cl/Ni 3 S 2 @graphene, Adv. Energy Mater 6 (2016) 1600137, https://doi.org/10.1002/aenm.201600137.
[123] Z. Yu, Z. Kang, Z. Hu, J. Lu, Z. Zhou, S. Jiao, Hexagonal NiS nanobelts as advanced cathode materials for rechargeable Al-ion batteries, Chem. Commun. 52 (2016) 10427–10430, https://doi.org/10.1039/c6cc05974k.
[124] T. Mori, Y. Orikasa, K. Nakanishi, C. Kezheng, M. Hattori, T. Ohta, Y. Uchimoto, Discharge/charge reaction mechanisms of FeS2 cathode material for aluminum rechargeable batteries at 55°C, J. Power Sources 313 (2016) 9–14, https://doi.org/10.1016/j.jpowsour.2016.02.062.
[125] S. Wang, S. Jiao, J. Wang, H.-S. Sen Chen, D. Tian, H. Lei, D.-N.N. Fang, High-performance aluminum-ion battery with CuS@C microsphere composite cathode, ACS Nano 11 (2017) 469–477, https://doi.org/10.1021/acsnano.6b06446.
[126] Y. Hu, D. Ye, B. Luo, H. Hu, X. Zhu, S. Wang, L. Li, S. Peng, L. Wang, A binder-free and free-standing cobalt Sulfide@Carbon nanotube cathode material for aluminum-ion batteries, Adv. Mater. 30 (2018) 1703824, https://doi.org/10.1002/adma.201703824.
[127] L. Geng, J.P. Scheifers, C. Fu, J. Zhang, B.P.T. Fokwa, J. Guo, Titanium sulfides as intercalation-type cathode materials for rechargeable aluminum batteries, ACS Appl. Mater. Interfaces 9 (2017) 21251–21257, https://doi.org/10.1021/acsami.7b04161.
[128] Y. Hu, B. Luo, D. Ye, X. Zhu, M. Lyu, L. Wang, An innovative freeze-dried reduced graphene oxide supported SnS 2 cathode active material for aluminum-ion batteries, Adv. Mater. 29 (2017) 1606132, https://doi.org/10.1002/adma.201606132.
[129] H. Li, H. Yang, Z. Sun, Y. Shi, H.-M. Cheng, F. Li, A highly reversible Co3S4 microsphere cathode material for aluminum-ion batteries, Nanomater. Energy 56 (2019) 100–108, https://doi.org/10.1016/j.nanoen.2018.11.045.
[130] L. Wu, R. Sun, F. Xiong, C. Pei, K. Han, C. Peng, Y. Fan, W. Yang, Q. An, L. Mai, A rechargeable aluminum-ion battery based on a VS2 nanosheet cathode, Phys. Chem. Chem. Phys. 20 (2018) 22563–22568, https://doi.org/10.1039/c8cp04772c.
[131] K. Liang, L. Ju, S. Koul, A. Kushima, Y. Yang, Self-supported tin sulfide porous films for flexible aluminum-ion batteries, Adv. Energy Mater. 9 (2019) 1–7, https://doi.org/10.1002/aenm.201802543.
[132] J. Tu, M. Wang, X. Xiao, H. Lei, S. Jiao, Nickel phosphide nanosheets supported on reduced graphene oxide for enhanced aluminum-ion batteries, ACS Sustain. Chem. Eng. 7 (2019) 6004–6012, https://doi.org/10.1021/acssuschemeng.8b06063.
[133] H. Lei, M. Wang, J. Tu, S. Jiao, Single-crystal and hierarchical VSe2 as an aluminum-ion battery cathode, Sustain. Energy Fuels 3 (2019) 2717–2724, https://doi.org/10.1039/c9se00288j.
[134] Z. Li, C. Gao, J. Zhang, A. Meng, H. Zhang, L. Yang, Mountain-like nanostructured 3D Ni3S2 on Ni foam for rechargeable aluminum battery and its theoretical analysis on charge/discharge mechanism, J. Alloys Compd. 798 (2019) 500–506, https://doi.org/10.1016/j.jallcom.2019.05.270.
[135] W. Yang, H. Lu, Y. Cao, B. Xu, Y. Deng, W. Cai, Flexible free-standing MoS 2/carbon nanofibers composite cathode for rechargeable aluminum-ion batteries, ACS Sustain. Chem. Eng. 7 (2019) 4861–4867, https://doi.org/10.1021/acssuschemeng.8b05292.
[136] Z. Li, B. Niu, J. Liu, J. Li, F. Kang, Rechargeable aluminum-ion battery based on MoS 2 microsphere cathode, ACS Appl. Mater. Interfaces 10 (2018) 9451–9459, https://doi.org/10.1021/acsami.8b00100.
[137] W. Yang, H. Lu, Y. Cao, P. Jing, X. Hu, H. Yu, A flexible free-standing cathode based on graphene-like MoSe2 nanosheets anchored on N-doped carbon nanofibers for rechargeable aluminum-ion batteries, Ionics 26 (2020) 3405–3413, https://doi.org/10.1007/s11581-020-03476-x.
[138] Z. Hu, K. Zhi, Q. Li, Z. Zhao, H. Liang, X. Liu, J. Huang, C. Zhang, H. Li, X. Guo, Two-dimensionally porous cobalt sulfide nanosheets as a high-performance cathode for aluminum-ion batteries, J. Power Sources 440 (2019) 227147, https://doi.org/10.1016/j.jpowsour.2019.227147.
[139] W. Xing, X. Li, T. Cai, Y. Zhang, P. Bai, J. Xu, H. Hu, M. Wu, Q. Xue, Y. Zhao, J. Zhou, S. Zhuo, X. Gao, Z. Yan, Layered double hydroxides derived NiCo-sulfide as a cathode material for aluminum ion batteries, Electrochim. Acta 344 (2020) 136174, https://doi.org/10.1016/j.electacta.2020.136174.
[140] W. Yang, H. Lu, Y. Cao, P. Jing, Single-/few-layered ultrasmall WS2 nanoplates embedded in nitrogen-doped carbon nanofibers as a cathode for rechargeable aluminum batteries, J. Power Sources 441 (2019) 227173, https://doi.org/10.1016/j.jpowsour.2019.227173.
[141] B. Lee, H.R. Lee, T. Yim, J.H. Kim, J.G. Lee, K.Y. Chung, B.W. Cho, S.H. Oh, Investigation on the structural evolutions during the insertion of aluminum ions into Mo 6 S 8 chevrel phase, J. Electrochem. Soc. 163 (2016) A1070–A1076, https://doi.org/10.1149/2.0011607jes.

[142] L. Geng, G. Lv, X. Xing, J. Guo, Reversible electrochemical intercalation of aluminum in Mo6S8, Chem. Mater. 27 (2015) 4926–4929, https://doi.org/10.1021/acs.chemmater.5b01918.
[143] K. Zhang, T.H. Lee, J.H. Cha, H.W. Jang, J.W. Choi, M. Mahmoudi, M. Shokouhimehr, Metal-organic framework-derived metal oxide nanoparticles@reduced graphene oxide composites as cathode materials for rechargeable aluminium-ion batteries, Sci. Rep. 9 (2019) 4–11, https://doi.org/10.1038/s41598-019-50156-6.
[144] X. Huo, X. Wang, Z. Li, J. Liu, J. Li, Two-dimensional composite of D-Ti3C2T: X@S@TiO2 (MXene) as the cathode material for aluminum-ion batteries, Nanoscale 12 (2020) 3387–3399, https://doi.org/10.1039/c9nr09944a.
[145] A. Vahidmohammadi, A. Hadjikhani, S. Shahbazmohamadi, M. Beidaghi, Two-Dimensional vanadium carbide (MXene) as a high-capacity cathode material for rechargeable aluminum batteries, ACS Nano 11 (2017) 11135–11144, https://doi.org/10.1021/acsnano.7b05350.
[146] T. Schoetz, B. Craig, C. Ponce de Leon, A. Bund, M. Ueda, C.T.J. Low, Aluminium-poly(3,4-ethylenedioxythiophene) rechargeable battery with ionic liquid electrolyte, J. Energy Storage 28 (2020) 101176, https://doi.org/10.1016/j.est.2019.101176.
[147] M. Walter, K.V. Kravchyk, C. Böfer, R. Widmer, M.V. Kovalenko, Polypyrenes as high-performance cathode materials for aluminum batteries, Adv. Mater. 30 (2018) 1–6, https://doi.org/10.1002/adma.201705644.
[148] D.J. Yoo, J.W. Choi, Elucidating the extraordinary rate and cycling performance of phenanthrenequinone in aluminum-complex-ion batteries, J. Phys. Chem. Lett. 11 (2020) 2384–2392, https://doi.org/10.1021/acs.jpclett.0c00324.
[149] J. Bitenc, N. Lindahl, A. Vizintin, M.E. Abdelhamid, R. Dominko, P. Johansson, Concept and electrochemical mechanism of an Al metal anode – organic cathode battery, Energy Storage Mater 24 (2020) 379–383, https://doi.org/10.1016/j.ensm.2019.07.033.
[150] S. Zhao, H. Chen, J. Li, J. Zhang, Synthesis of polythiophene/graphite composites and their enhanced electrochemical performance for aluminum ion batteries, New J. Chem. 43 (2019) 15014–15022, https://doi.org/10.1039/c9nj03626a.
[151] D.J. Kim, D.-J. Yoo, M.T. Otley, A. Prokofjevs, C. Pezzato, M. Owczarek, S.J. Lee, J.W. Choi, J.F. Stoddart, Rechargeable aluminium organic batteries, Nat. Energy. 4 (2019) 51–59, https://doi.org/10.1038/s41560-018-0291-0.
[152] K. Zhang, T.H. Lee, B. Bubach, H.W. Jang, M. Ostadhassan, J.W. Choi, M. Shokouhimehr, Graphite carbon-encapsulated metal nanoparticles derived from Prussian blue analogs growing on natural loofa as cathode materials for rechargeable aluminum-ion batteries, Sci. Rep. 9 (2019) 1–9, https://doi.org/10.1038/s41598-019-50154-8.
[153] S. Wang, K.V. Kravchyk, S. Pigeot-Rémy, W. Tang, F. Krumeich, M. Wörle, M. I. Bodnarchuk, S. Cassaignon, O. Durupthy, S. Zhao, C. Sanchez, M.V. Kovalenko, Anatase TiO 2 nanorods as cathode materials for aluminum-ion batteries, ACS Appl. Nano Mater. 2 (2019) 6428–6435, https://doi.org/10.1021/acsanm.9b01391.
[154] G. Li, J. Tu, M. Wang, S. Jiao, Cu3P as a novel cathode material for rechargeable aluminum-ion batteries, J. Mater. Chem. A. 7 (2019) 8368–8375, https://doi.org/10.1039/c9ta00762h.
[155] Q. Yan, Y. Shen, Y. Miao, M. Wang, M. Yang, X. Zhao, Vanadium oxychloride as cathode for rechargeable aluminum batteries, J. Alloys Compd. 806 (2019) 1109–1115, https://doi.org/10.1016/j.jallcom.2019.07.324.
[156] Z. Li, J. Li, F. Kang, 3D hierarchical AlV 3 O 9 microspheres as a cathode material for rechargeable aluminum-ion batteries, Electrochim. Acta 298 (2019) 288–296, https://doi.org/10.1016/j.electacta.2018.12.095.
[157] A.M. Diem, B. Fenk, J. Bill, Z. Burghard, Binder-free v2o5 cathode for high energy density rechargeable aluminum-ion batteries, Nanomaterials 10 (2020) 1–15, https://doi.org/10.3390/nano10020247.
[158] S. Gu, H. Wang, C. Wu, Y. Bai, H. Li, F. Wu, Confirming reversible Al3+ storage mechanism through intercalation of Al3+ into V2O5 nanowires in a rechargeable aluminum battery, Energy Storage Mater 6 (2017) 9–17, https://doi.org/10.1016/j.ensm.2016.09.001.
[159] Z. Yu, J. Tu, C. Wang, S. Jiao, A rechargeable Al/graphite battery based on AlCl 3/1-butyl-3-methylimidazolium chloride ionic liquid electrolyte, Chemistry 4 (2019) 3018–3024, https://doi.org/10.1002/slct.201900374.
[160] G.A. Elia, N.A. Kyeremateng, K. Marquardt, R. Hahn, An aluminum/graphite battery with ultra-high rate capability, Batter. Supercaps. 2 (1) (2018) 83–90, https://doi.org/10.1002/batt.201800114.
[161] G. Greco, D. Tatchev, A. Hoell, M. Krumrey, S. Raoux, R. Hahn, G.A. Elia, Influence of the electrode nano/microstructure on the electrochemical properties of graphite in aluminum batteries, J. Mater. Chem. A. 6 (2018) 22673–22680, https://doi.org/10.1039/C8TA08319C.
[162] G. Zhu, M. Angell, C.J. Pan, M.C. Lin, H. Chen, C.J. Huang, J. Lin, A.J. Achazi, P. Kaghazchi, B.J. Hwang, H. Dai, Rechargeable aluminum batteries: effects of cations in ionic liquid electrolytes, RSC Adv. 9 (2019) 11322–11330, https://doi.org/10.1039/C9RA00765B.
[163] C. Yang, S. Wang, X. Zhang, Q. Zhang, W. Ma, S. Yu, G. Sun, Substituent effect of imidazolium ionic liquid: a potential strategy for high coulombic efficiency Al battery, J. Phys. Chem. C 123 (2019) 11522–11528, https://doi.org/10.1021/acs.jpcc.9b02318.
[164] C. Xu, J. Li, H. Chen, J. Zhang, Benzyltriethylammonium chloride electrolyte for high-performance Al-ion batteries, ChemNanoMat 5 (2019) 1367–1372, https://doi.org/10.1002/cnma.201900490.
[165] S. Xia, X.-M. Zhang, K. Huang, Y.-L. Chen, Y.-T. Wu, Ionic liquid electrolytes for aluminium secondary battery: influence of organic solvents, J. Electroanal. Chem. 757 (2015) 167–175, https://doi.org/10.1016/j.jelechem.2015.09.022.
[166] F. Gan, K. Chen, N. Li, Y. Wang, Y. Shuai, X. He, Low cost ionic liquid electrolytes for rechargeable aluminum/graphite batteries, Ionics 25 (2019) 4243–4249, https://doi.org/10.1007/s11581-019-02983-w.
[167] H. Xu, T. Bai, H. Chen, F. Guo, J. Xi, T. Huang, S. Cai, X. Chu, J. Ling, W. Gao, Z. Xu, C. Gao, Low-cost AlCl3/Et3NHCl electrolyte for high-performance aluminum-ion battery, Energy Storage Mater 17 (2019) 38–45, https://doi.org/10.1016/j.ensm.2018.08.003.
[168] X. Dong, H. Xu, H. Chen, L. Wang, J. Wang, W. Fang, C. Chen, M. Salman, Z. Xu, C. Gao, Commercial expanded graphite as high-performance cathode for low-cost aluminum-ion battery, Carbon N. Y. 148 (2019) 134–140, https://doi.org/10.1016/j.carbon.2019.03.080.
[169] C. Xu, S. Zhao, Y. Du, W. Zhang, P. Li, H. Jin, Y. Zhang, Z. Wang, J. Zhang, A high capacity aluminum-ion battery based on imidazole hydrochloride electrolyte, ChemElectroChem 6 (2019) 3350–3354, https://doi.org/10.1002/celc.201900883.
[170] V.A. Elterman, P.Y. Shevelin, D.L. Chizhov, L.A. Yolshina, E.A. Il'ina, A. V. Borozdin, M.I. Kodess, M.A. Ezhikova, G.L. Rusinov, Development of a novel 1-trifluoroacetyl piperidine-based electrolyte for aluminum ion battery, Electrochim. Acta 323 (2019) 134806, https://doi.org/10.1016/j.electacta.2019.134806.
[171] S. Liu, X. Zhang, S. He, Y. Tang, J. Wang, B. Wang, S. Zhao, H. Su, Y. Ren, L. Zhang, J. Huang, H. Yu, K. Amine, An advanced high energy-efficiency rechargeable aluminum-selenium battery, Nanomater. Energy 66 (2019) 104159, https://doi.org/10.1016/j.nanoen.2019.104159.
[172] H. Yang, L. Yin, J. Liang, Z. Sun, Y. Wang, H. Li, K. He, L. Ma, Z. Peng, S. Qiu, C. Sun, H.-M.M. Cheng, F. Li, An aluminum-sulfur battery with a fast kinetic response, Angew. Chem. Int. Ed. 57 (2018) 1898–1902, https://doi.org/10.1002/anie.201711328.
[173] M. Latha, J. Vatsala Rani, WS 2/graphene composite as cathode for rechargeable aluminum-dual ion battery, J. Electrochem. Soc. 167 (2020), https://doi.org/10.1149/2.0012007jes, 070501.
[174] M. Angell, C.-J. Pan, Y. Rong, C. Yuan, M.-C. Lin, B.-J. Hwang, H. Dai, High Coulombic efficiency aluminum-ion battery using an AlCl 3 -urea ionic liquid analog electrolyte, Proc. Natl. Acad. Sci. Unit. States Am. 114 (2017) 834–839, https://doi.org/10.1073/pnas.1619795114.
[175] C. Liu, W. Chen, Z. Wu, B. Gao, X. Hu, Z. Shi, Z. Wang, Density, viscosity and electrical conductivity of AlCl3-amide ionic liquid analogues, J. Mol. Liq. 247 (2017) 57–63, https://doi.org/10.1016/j.molliq.2017.09.091.
[176] H. Jiao, C. Wang, J. Tu, D. Tian, S. Jiao, A rechargeable Al-ion battery: Al/molten AlCl3-urea/graphite, Chem. Commun. 53 (2017) 2331–2334, https://doi.org/10.1039/c6cc09825h.
[177] M. Angell, G. Zhu, M. Lin, Y. Rong, H. Dai, Ionic liquid analogs of AlCl 3 with urea derivatives as electrolytes for aluminum batteries, Adv. Funct. Mater. 30 (2020) 1901928, https://doi.org/10.1002/adfm.201901928.
[178] K.L. Ng, M. Malik, E. Buch, T. Glossmann, A. Hintennach, G. Azimi, A low-cost rechargeable aluminum/natural graphite battery utilizing urea-based ionic liquid analog, Electrochim. Acta 327 (2019) 135031, https://doi.org/10.1016/j.electacta.2019.135031.
[179] C.-J. Pan, C. Yuan, G. Zhu, Q. Zhang, C.-J. Huang, M.-C. Lin, M. Angell, B.-J. Hwang, P. Kaghazchi, H. Dai, An operando X-ray diffraction study of chloroaluminate anion-graphite intercalation in aluminum batteries, Proc. Natl. Acad. Sci. Unit. States Am. 115 (2018) 5670–5675, https://doi.org/10.1073/pnas.1803576115.
[180] W. Chu, X. Zhang, J. Wang, S. Zhao, S. Liu, H. Yu, A low-cost deep eutectic solvent electrolyte for rechargeable aluminum-sulfur battery, Energy Storage Mater 22 (2019) 418–423, https://doi.org/10.1016/j.ensm.2019.01.025.
[181] C. Xu, W. Zhang, P. Li, S. Zhao, Y. Du, H. Jin, Y. Zhang, Z. Wang, J. Zhang, High-performance aluminum-ion batteries based on AlCl3/caprolactam electrolytes, Sustain. Energy Fuels 4 (2019) 121–127, https://doi.org/10.1039/c9se00941h.
[182] C. Li, J. Patra, J. Li, P.C. Rath, M.H. Lin, J.K. Chang, A novel moisture-insensitive and low-corrosivity ionic liquid electrolyte for rechargeable aluminum batteries, Adv. Funct. Mater. 30 (2020) 1–10, https://doi.org/10.1002/adfm.201909565.
[183] M. Chiku, T. Kunisawa, E. Higuchi, H. Inoue, Copper chloride as a conversion-type positive electrode for rechargeable aluminum batteries, RSC Adv. 9 (2019) 41475–41480, https://doi.org/10.1039/c9ra09158k.
[184] M. Chiku, H. Takeda, S. Matsumura, E. Higuchi, H. Inoue, Amorphous vanadium oxide/carbon composite positive electrode for rechargeable aluminum battery, ACS Appl. Mater. Interfaces 7 (2015) 24385–24389, https://doi.org/10.1021/acsami.5b06420.
[185] J. Li, J. Tu, H. Jiao, C. Wang, S. Jiao, Ternary AlCl 3 -Urea-[EMIm]Cl ionic liquid electrolyte for rechargeable aluminum-ion batteries, J. Electrochem. Soc. 164 (2017) A3093–A3100, https://doi.org/10.1149/2.0811713jes.
[186] X.-G. Sun, Y. Fang, X. Jiang, K. Yoshii, T. Tsuda, S. Dai, Polymer gel electrolytes for application in aluminum deposition and rechargeable aluminum ion batteries, Chem. Commun. 52 (2016) 292–295, https://doi.org/10.1039/c5cc06643c.
[187] S. Song, M. Kotobuki, F. Zheng, Q. Li, C. Xu, Y. Wang, W.D.Z. Li, N. Hu, L. Lu, Al conductive hybrid solid polymer electrolyte, Solid State Ionics 300 (2017) 165–168, https://doi.org/10.1016/j.ssi.2016.12.023.
[188] M. Kotobuki, L. Lu, S.V. Savilov, S.M. Aldoshin, Poly(vinylidene fluoride)-based Al ion conductive solid polymer electrolyte for Al battery, J. Electrochem. Soc. 164 (2017) A3868–A3875, https://doi.org/10.1149/2.1601714jes.
[189] Z. Yu, S. Jiao, S. Li, X. Chen, W.-L.L. Song, T. Teng, J. Tu, H.-S. Sen Chen, G. Zhang, D.-N.N. Fang, Flexible stable solid-state Al-ion batteries, Adv. Funct. Mater. 29 (2019) 1–9, https://doi.org/10.1002/adfm.201806799.

[190] Z. Yu, S. Jiao, J. Tu, W.L. Song, H. Lei, H. Jiao, H. Chen, D. Fang, Gel electrolytes with a wide potential window for high-rate Al-ion batteries, J. Mater. Chem. A. 7 (2019) 20348–20356, https://doi.org/10.1039/c9ta06815e.
[191] T. Schoetz, O. Leung, C.P. de Leon, C. Zaleski, I. Efimov, Aluminium deposition in EMImCl-AlCl 3 ionic liquid and ionogel for improved aluminium batteries, J. Electrochem. Soc. 167 (2020), https://doi.org/10.1149/1945-7111/ab7573, 040516.
[192] W. Pan, Y. Wang, Y. Zhang, H.Y.H. Kwok, M. Wu, X. Zhao, D.Y.C. Leung, A low-cost and dendrite-free rechargeable aluminium-ion battery with superior performance, J. Mater. Chem. A. 7 (2019) 17420–17425, https://doi.org/10.1039/C9TA05207K.
[193] H. Wang, S. Gu, Y. Bai, S. Chen, F. Wu, C. Wu, High-voltage and noncorrosive ionic liquid electrolyte used in rechargeable aluminum battery, ACS Appl. Mater. Interfaces 8 (2016) 27444–27448, https://doi.org/10.1021/acsami.6b10579.
[194] L.D. Reed, A. Arteaga, E.J. Menke, A combined experimental and computational study of an aluminum triflate/diglyme electrolyte, J. Phys. Chem. B 119 (2015) 12677–12681, https://doi.org/10.1021/acs.jpcb.5b08501.
[195] T. Mandai, P. Johansson, Al conductive haloaluminate-free non-aqueous room-temperature electrolytes, J. Mater. Chem. A. 3 (2015) 12230–12239, https://doi.org/10.1039/C5TA01760B.
[196] T. Mandai, P. Johansson, Haloaluminate-free cationic aluminum complexes: structural characterization and physicochemical properties, J. Phys. Chem. C 120 (2016) 21285–21292, https://doi.org/10.1021/acs.jpcc.6b07235.
[197] M. Chiku, S. Matsumura, H. Takeda, E. Higuchi, H. Inoue, Aluminum bis (trifluoromethanesulfonyl)imide as a chloride-free electrolyte for rechargeable aluminum batteries, J. Electrochem. Soc. 164 (2017) A1841–A1844, https://doi.org/10.1149/2.0701709jes.
[198] Z. Hu, Y. Guo, H. Jin, H. Ji, L.-J. Wan, A rechargeable aqueous aluminum–sulfur battery through acid activation in water-in-salt electrolyte, Chem. Commun. 56 (2020) 2023–2026, https://doi.org/10.1039/C9CC08415K.
[199] A. Zhou, L. Jiang, J. Yue, Y. Tong, Q. Zhang, Z. Lin, B. Liu, C. Wu, L. Suo, Y.S. Hu, H. Li, L. Chen, Water-in-Salt electrolyte promotes high-capacity FeFe(CN)6 cathode for aqueous Al-ion battery, ACS Appl. Mater. Interfaces 11 (2019) 41356–41362, https://doi.org/10.1021/acsami.9b14149.
[200] Q. Zhao, L. Liu, J. Yin, J. Zheng, D. Zhang, J. Chen, L.A. Archer, Proton intercalation/de-intercalation dynamics in vanadium oxides for aqueous aluminum electrochemical cells, Angew. Chem. Int. Ed. 59 (2020) 3048–3052, https://doi.org/10.1002/anie.201912634.
[201] N.V. Plechkova, K.R. Seddon, Applications of ionic liquids in the chemical industry, Chem. Soc. Rev. 37 (2008) 123–150, https://doi.org/10.1039/B006677J.
[202] F.H. Hurley, T.P. WIer, The electrodeposition of aluminum from nonaqueous solutions at room temperature, J. Electrochem. Soc. 98 (1951) 207, https://doi.org/10.1149/1.2778133.
[203] J. Robinson, R.A. Osteryoung, An electrochemical and spectroscopic study of some aromatic hydrocarbons in the room temperature molten salt system aluminum chloride-n-butylpyridinium chloride, J. Am. Chem. Soc. 101 (1979) 323–327, https://doi.org/10.1021/ja00496a008.
[204] J.S. Wilkes, J.A. Levisky, R.A. Wilson, C.L. Hussey, Dialkylimidazolium chloroaluminate melts: a new class of room-temperature ionic liquids for electrochemistry, spectroscopy and synthesis, Inorg. Chem. 21 (1982) 1263–1264, https://doi.org/10.1021/ic00133a078.
[205] P.K. Lai, M. Skyllas-Kazacos, Aluminium deposition and dissolution in aluminium chloride—n-butylpyridinium chloride melts, Electrochim. Acta 32 (1987) 1443–1449, https://doi.org/10.1016/0013-4686(87)85083-1.
[206] L.P. Davis, C.J. Dymek, J.J.P. Stewart, H.P. Clark, W.J. Lauderdale, MNDO calculations of ions in chloroaluminate molten salts, J. Am. Chem. Soc. 107 (1985) 5041–5046, https://doi.org/10.1021/ja00304a003.
[207] Y. Chao-Cheng, Electrodeposition of aluminum in molten AlCl3-n-butylpyridinium chloride electrolyte, Mater. Chem. Phys. 37 (1994) 355–361, https://doi.org/10.1016/0254-0584(94)90175-9.
[208] Y. Zhao, T.J.J. VanderNoot, Review: electrodeposition of aluminium from nonaqueous organic electrolytic systems and room temperature molten salts, Electrochim. Acta 42 (1997) 3–13, https://doi.org/10.1016/0013-4686(96)00080-1.
[209] S. Takahashi, N. Koura, S. Kohara, M.-L. Saboungi, L.A. Curtiss, Technological and scientific issues of room-temperature molten salts, Plasma Ions 2 (1999) 91–105, https://doi.org/10.1016/S1288-3255(99)00105-7.
[210] T. Jiang, M.J.J. Chollier Brym, G. Dubé, A. Lasia, G.M.M. Brisard, Electrodeposition of aluminium from ionic liquids: Part I-electrodeposition and surface morphology of aluminium from aluminium chloride (AlCl3)-1-ethyl-3-methylimidazolium chloride ([EMIm]Cl) ionic liquids, Surf. Coating. Technol. 201 (2006) 1–9, https://doi.org/10.1016/j.surfcoat.2005.10.046.
[211] S. Schaltin, M. Ganapathi, K. Binnemans, J. Fransaer, Modeling of aluminium deposition from chloroaluminate ionic liquids, J. Electrochem. Soc. 158 (2011) D634, https://doi.org/10.1149/1.3623781.
[212] J.S. Wilkes, M.J. Zaworotko, Air and water stable 1-ethyl-3-methylimidazolium based ionic liquids, J. Chem. Soc. Chem. Commun. (1992) 965, https://doi.org/10.1039/c39920000965.
[213] Handbook of metallurgical process design, in: L. Xie, K. Funatani, G. Totten (Eds.), CRC Press, 2004, https://doi.org/10.1201/9780203970928.
[214] H.M.A. Abood, A.P. Abbott, A.D. Ballantyne, K.S. Ryder, Do all ionic liquids need organic cations? Characterisation of [AlCl 2·nAmide]+ AlCl4- and comparison with imidazolium based systems, Chem. Commun. 47 (2011) 3523–3525, https://doi.org/10.1039/c0cc04989a.
[215] Y. Fang, K. Yoshii, X. Jiang, X.-G. Sun, T. Tsuda, N. Mehio, S. Dai, An AlCl3 based ionic liquid with a neutral substituted pyridine ligand for electrochemical deposition of aluminum, Electrochim. Acta 160 (2015) 82–88, https://doi.org/10.1016/j.electacta.2015.02.020.
[216] G. Pulletikurthi, B. Bödecker, A. Borodin, B. Weidenfeller, F. Endres, Electrodeposition of Al from a 1-butylpyrrolidine-AlCl3 ionic liquid, Prog. Nat. Sci. Mater. Int. 25 (2015) 603–611, https://doi.org/10.1016/j.pnsc.2015.11.003.
[217] Y. Fang, X. Jiang, X.-G. Sun, S. Dai, New ionic liquids based on the complexation of dipropyl sulfide and AlCl 3 for electrodeposition of aluminum, Chem. Commun. 51 (2015) 13286–13289, https://doi.org/10.1039/C5CC05233E.
[218] Y. Bian, Y. Li, Z. Yu, H. Chen, K. Du, C. Qiu, G. Zhang, Z. Lv, M.-C. Lin, Using an AlCl 3/urea ionic liquid analog electrolyte for improving the lifetime of aluminum-sulfur batteries, ChemElectroChem 5 (2018) 3607–3611, https://doi.org/10.1002/celc.201801198.
[219] C.H. Ko, J.M. Stuve, R.R. Brown, Bureau of Mines Report of Investigation, Low-Temperature Heat Capacities and Enthalpy of Formation of Aluminum Sulfide (Al2S3), Bureau of, 1976.
[220] J.J. Vajo, A.F. Gross, P. Liu, J. Hicks-Garner, E. Sherman, S. Van Atta, US Patent N° 8 (853 B1) (2014) 715.
[221] C.H. Tseng, J.K. Chang, J.R. Chen, W.T. Tsai, M.J. Deng, I.W. Sun, Corrosion behaviors of materials in aluminum chloride-1-ethyl-3- methylimidazolium chloride ionic liquid, Electrochem. Commun. 12 (2010) 1091–1094, https://doi.org/10.1016/j.elecom.2010.05.036.
[222] P.C. Lin, I.W. Sun, J.K. Chang, C.J. Su, J.C. Lin, Corrosion characteristics of nickel, copper, and stainless steel in a Lewis neutral chloroaluminate ionic liquid, Corrosion Sci. 53 (2011) 4318–4323, https://doi.org/10.1016/j.corsci.2011.08.047.
[223] Q. Zhang, Y. Hua, Z. Zhou, Corrosion properties of copper, nickel, and titanium in alkylimidazolium chloroaluminate based ionic liquids, Int. J. Electrochem. Sci. 8 (2013) 10239–10249.
[224] J.P.M. Veder, M.D. Horne, T. Rüther, A.M. Bond, T. Rodopoulos, Aluminium oxidation at high anodic potentials in an AlCl 3-containing air- and water-stable ionic liquid solution, Electrochem. Commun. 37 (2013) 68–70, https://doi.org/10.1016/j.elecom.2013.10.015.
[225] Y.C. Wang, T.C. Lee, J.Y. Lin, J.K. Chang, C.M. Tseng, Corrosion properties of metals in dicyanamide-based ionic liquids, Corrosion Sci. 78 (2014) 81–88, https://doi.org/10.1016/j.corsci.2013.09.002.
[226] B. Dilasari, Y. Jung, J. Sohn, S. Kim, K. Kwon, Review on corrosion behavior of metallic materials in room temperature ionic liquids, Int. J. Electrochem. Sci. 11 (2016) 1482–1495.
[227] L.D. Reed, E. Menke, The roles of V2O5 and stainless steel in rechargeable Al-ion batteries, J. Electrochem. Soc. 160 (2013) A915–A917, https://doi.org/10.1149/2.114306jes.
[228] J. Shi, J. Zhang, J. Guo, Avoiding pitfalls in rechargeable aluminum batteries research, ACS Energy Lett 4 (2019) 2124–2129, https://doi.org/10.1021/acsenergylett.9b01285.
[229] S. Wang, K.V. Kravchyk, A.N. Filippin, U. Müller, A.N. Tiwari, S. Buecheler, M. I. Bodnarchuk, M.V. Kovalenko, Aluminum chloride-graphite batteries with flexible current collectors prepared from earth-abundant elements, Adv. Sci. 5 (2018) 1700712, https://doi.org/10.1002/advs.201700712.
[230] X. Wen, Y. Liu, A. Jadhav, J. Zhang, D. Borchardt, J. Shi, B.M. Wong, B. Sanyal, R. J. Messinger, J. Guo, Materials compatibility in rechargeable aluminum batteries: chemical and electrochemical properties between vanadium pentoxide and chloroaluminate ionic liquids, Chem. Mater. 31 (2019) 7238–7247, https://doi.org/10.1021/acs.chemmater.9b01556.
[231] H.J.T. Ellingham, Reducibility of oxides and sulfides in metallurgical processes, J Soc Chem Ind 63 (1944) 125–133.
[232] G.A. Elia, J.-B. Ducros, D. Sotta, V. Delhorbe, A. Brun, K. Marquardt, R. Hahn, Polyacrylonitrile separator for high-performance aluminum batteries with improved interface stability, ACS Appl. Mater. Interfaces 9 (2017) 38381–38389, https://doi.org/10.1021/acsami.7b09378.
[233] Y. Nakayama, Y. Senda, H. Kawasaki, N. Koshitani, S. Hosoi, Y. Kudo, H. Morioka, M. Nagamine, Sulfone-based electrolytes for aluminium rechargeable batteries, Phys. Chem. Chem. Phys. 17 (2015) 5758–5766, https://doi.org/10.1039/c4cp02183e.
[234] Z. Rong, R. Malik, P. Canepa, G. Sai Gautam, M. Liu, A. Jain, K. Persson, G. Ceder, Materials design rules for multivalent ion mobility in intercalation structures, Chem. Mater. 27 (2015) 6016–6021, https://doi.org/10.1021/acs.chemmater.5b02342.
[235] L. Zhang, L. Chen, H. Luo, X. Zhou, Z. Liu, Large-sized few-layer graphene enables an ultrafast and long-life aluminum-ion battery, Adv. Energy Mater. 7 (2017) 1700034, https://doi.org/10.1002/aenm.201700034.
[236] J. Qiao, H. Zhou, Z. Liu, H. Wen, J. Yang, Defect-free soft carbon as cathode material for Al-ion batteries, Ionics 25 (2019) 1235–1242, https://doi.org/10.1007/s11581-019-02896-8.
[237] Y. Hu, S. Debnath, H. Hu, B. Luo, X. Zhu, S. Wang, M. Hankel, D.J. Searles, L. Wang, Unlocking the potential of commercial carbon nanofibers as free-standing positive electrodes for flexible aluminum ion batteries, J. Mater. Chem. A. 7 (2019) 15123–15130, https://doi.org/10.1039/c9ta04085d.
[238] D. Muñoz-Torrero, J. Palma, R. Marcilla, E. Ventosa, Al-ion battery based on semisolid electrodes for higher specific energy and lower cost, ACS Appl. Energy Mater. 3 (2020) 2285–2289, https://doi.org/10.1021/acsaem.9b02253.
[239] H. Xu, H. Chen, H. Lai, Z. Li, X. Dong, S. Cai, X. Chu, C. Gao, Capacitive charge storage enables an ultrahigh cathode capacity in aluminum-graphene battery, J. Energy Chem. 45 (2020) 40–44, https://doi.org/10.1016/j.jechem.2019.09.025.

[240] H. Hu, T. Cai, P. Bai, J. Xu, S. Ge, H. Hu, M. Wu, Q. Xue, Z. Yan, X. Gao, W. Xing, Small graphite nanoflakes as an advanced cathode material for aluminum ion batteries, Chem. Commun. 56 (2020) 1593–1596, https://doi.org/10.1039/c9cc06895c.

[241] X. Yu, B. Wang, D. Gong, Z. Xu, B. Lu, Graphene nanoribbons on highly porous 3D graphene for high-capacity and ultrastable Al-ion batteries, Adv. Mater. 29 (2017) 1604118, https://doi.org/10.1002/adma.201604118.

[242] S.C. Jung, Y.J. Kang, D.J. Yoo, J.W. Choi, Y.K. Han, Flexible few-layered graphene for the ultrafast rechargeable aluminum-ion battery, J. Phys. Chem. C 120 (2016) 13384–13389, https://doi.org/10.1021/acs.jpcc.6b03657.

[243] P. Wang, H. Chen, N. Li, X. Zhang, S. Jiao, W.-L. Song, D. Fang, Dense graphene papers: toward stable and recoverable Al-ion battery cathodes with high volumetric and areal energy and power density, Energy Storage Mater 13 (2018) 103–111, https://doi.org/10.1016/j.ensm.2018.01.001.

[244] C.-Y. Chen, T. Tsuda, S. Kuwabata, C.L. Hussey, Rechargeable aluminum batteries utilizing a chloroaluminate inorganic ionic liquid electrolyte, Chem. Commun. 54 (2018) 4164–4167, https://doi.org/10.1039/C8CC00113H.

[245] Z. Li, J. Liu, B. Niu, J. Li, F. Kang, A novel graphite-graphite dual ion battery using an AlCl 3 -[EMIm]Cl liquid electrolyte, Small 14 (2018) 1800745, https://doi.org/10.1002/smll.201800745.

[246] Z. Liu, J. Wang, H. Ding, S. Chen, X. Yu, B. Lu, Carbon nanoscrolls for aluminum battery, ACS Nano 12 (2018) 8456–8466, https://doi.org/10.1021/acsnano.8b03961.

[247] J. Smajic, A. Alazmi, N. Batra, T. Palanisamy, D.H. Anjum, P.M.F.J. Costa, Mesoporous reduced graphene oxide as a high capacity cathode for aluminum batteries, Small 14 (2018) 1803584, https://doi.org/10.1002/smll.201803584.

[248] J. Wang, X. Zhang, W. Chu, S. Liu, H. Yu, A sub-100 ° C aluminum ion battery based on a ternary inorganic molten salt, Chem. Commun. 55 (2019) 2138–2141, https://doi.org/10.1039/C8CC09677E.

[249] H. Yang, L. Yin, J. Liang, Z. Sun, Y. Wang, H. Li, K. He, L. Ma, Z. Peng, S. Qiu, C. Sun, H.-M. Cheng, F. Li, An aluminum-sulfur battery with a fast kinetic response, Angew. Chem. 130 (2018) 1916–1920, https://doi.org/10.1002/ange.201711328.

[250] P. Bhauriyal, S. Das, B. Pathak, Theoretical insights into the charge and discharge processes in aluminum–sulfur batteries, J. Phys. Chem. C 124 (21) (2020) 11317–11324, https://doi.org/10.1021/acs.jpcc.0c01358, acs.jpcc.0c01358.

[251] W. Wang, Z. Cao, G.A. Elia, Y. Wu, W. Wahyudi, E. Abou-Hamad, A.-H. Emwas, L. Cavallo, L.-J. Li, J. Ming, Recognizing the mechanism of sulfurized polyacrylonitrile cathode materials for Li–S batteries and beyond in Al–S batteries, ACS Energy Lett 3 (2018) 2899–2907, https://doi.org/10.1021/acsenergylett.8b01945.

[252] S. Wang, S. Huang, M. Yao, Y. Zhang, Z. Niu, Engineering Active Sites of Polyaniline for AlCl2+ Storage in Aluminum Battery, Angew. Chemie., 2020, https://doi.org/10.1002/ange.202002132.

[253] S. Wang, Z. Yu, J. Tu, J. Wang, D. Tian, Y. Liu, S. Jiao, A novel aluminum-ion battery: Al/AlCl3-[EMIm]Cl/Ni3S2@Graphene, Adv. Energy Mater 6 (2016), https://doi.org/10.1002/aenm.201600137.

[254] S. Ju, X. Chen, Z. Yang, G. Xia, X. Yu, Atomic scale understanding of aluminum intercalation into layered TiS2 and its electrochemical properties, J. Energy Chem. 43 (2020) 116–120, https://doi.org/10.1016/j.jechem.2019.09.003.

[255] T. Koketsu, J. Ma, B.J. Morgan, M. Body, C. Legein, W. Dachraoui, M. Giannini, A. Demortière, M. Salanne, F. Dardoize, H. Groult, O.J. Borkiewicz, K. W. Chapman, P. Strasser, D. Dambournet, Reversible magnesium and aluminium ions insertion in cation-deficient anatase TiO2, Nat. Mater. 16 (2017) 1142–1148, https://doi.org/10.1038/nmat4976.

[256] W. Tang, J. Xuan, H. Wang, S. Zhao, H. Liu, Aluminum intercalation and transport in TiO2(B) from first principles, J. Energy Storage. 24 (2019) 100800, https://doi.org/10.1016/j.est.2019.100800.

[257] S. Lee, S.C. Jung, Y.K. Han, Fe2CS2 MXene, A promising electrode for Al-ion batteries, Nanoscale 12 (2020) 5324–5331, https://doi.org/10.1039/c9nr08906c.

[258] W. Rüdorff, Kristallstruktur der Saureverbindungen des Graphits, Z. Phys. Chem. (1940) 42.

[259] N. Daumas, A. Herold, Relations between phase concept and reaction mechanics in graphite insertion compounds, Comptes Rendus Hebd. Des Seances L Acad. Des Sci. Ser. C. 268 (5) (1969) 373.

[260] Giuseppe Antonio Elia, Giorgia Greco, Paul H. Kamm, Francisco García–Moreno, Simone Raoux, Robert Hahn, Simultaneous X–ray diffraction and tomography operando investigation of aluminum/graphite batteries, Adv. Funct. Mater. (2020), https://doi.org/10.1002/adfm.202003913.

[261] P. Bhauriyal, A. Mahata, B. Pathak, Graphene-like carbon–nitride monolayer: a potential anode material for Na- and K-ion batteries, J. Phys. Chem. C 122 (2018) 2481–2489, https://doi.org/10.1021/acs.jpcc.7b09433.

[262] H. Wang, S. Gu, Y. Bai, S. Chen, N. Zhu, C. Wu, F. Wu, Anion-effects on electrochemical properties of ionic liquid electrolytes for rechargeable aluminum batteries, J. Mater. Chem. A. 3 (2015) 22677–22686, https://doi.org/10.1039/c5ta06187c.

[263] S. Zein El Abedin, E.M. Moustafa, R. Hempelmann, H. Natter, F. Endres, Electrodeposition of nano- and macrocrystalline aluminium in three different air and water stable ionic liquids, ChemPhysChem 7 (2006) 1535–1543, https://doi.org/10.1002/cphc.200600095.

[264] T. Jiang, M.J. Chollier Brym, G. Dubé, A. Lasia, G.M. Brisard, Electrodeposition of aluminium from ionic liquids: Part II - studies on the electrodeposition of aluminum from aluminum chloride (AlCl3) - trimethylphenylammonium chloride (TMPAC) ionic liquids, Surf. Coating. Technol. 201 (2006) 10–18, https://doi.org/10.1016/j.surfcoat.2005.12.024.

[265] A.P. Abbott, R.C. Harris, Y.T. Hsieh, K.S. Ryder, I.W. Sun, Aluminium electrodeposition under ambient conditions, Phys. Chem. Chem. Phys. 16 (2014) 14675–14681, https://doi.org/10.1039/c4cp01508h.

[266] A. Bakkar, V. Neubert, A new method for practical electrodeposition of aluminium from ionic liquids, Electrochem. Commun. 51 (2015) 113–116, https://doi.org/10.1016/j.elecom.2014.12.012.

[267] Y. Song, S. Jiao, J. Tu, J. Wang, Y. Liu, H. Jiao, X. Mao, Z. Guo, D.J. Fray, A long-life rechargeable Al ion battery based on molten salts, J. Mater. Chem. A. 5 (2017) 1282–1291, https://doi.org/10.1039/C6TA09829K.

[268] J. Tu, J. Wang, H. Zhu, S. Jiao, The molten chlorides for aluminum-graphite rechargeable batteries, J. Alloys Compd. 821 (2020) 153285, https://doi.org/10.1016/j.jallcom.2019.153285.

[269] E.L. Smith, A.P. Abbott, K.S. Ryder, Deep eutectic solvents (DESs) and their applications, Chem. Rev. 114 (2014) 11060–11082, https://doi.org/10.1021/cr300162p.

[270] F. Coleman, G. Srinivasan, M. Swadźba-Kwaśny, Liquid coordination complexes formed by the heterolytic cleavage of metal halides, Angew. Chem. Int. Ed. 52 (2013) 12582–12586, https://doi.org/10.1002/anie.201306267.

[271] M. Li, B. Gao, C. Liu, W. Chen, Z. Wang, Z. Shi, X. Hu, AlCl3/amide ionic liquids for electrodeposition of aluminum, J. Solid State Electrochem. 21 (2017) 469–476, https://doi.org/10.1007/s10008-016-3384-3.

[272] J. Maire, J. Mering, Chemistry and Physics of Carbon, 1970.

[273] M. Wissler, Graphite and carbon powders for electrochemical applications, J. Power Sources 156 (2006) 142–150, https://doi.org/10.1016/j.jpowsour.2006.02.064.

[274] A.C. Ferrari, Raman spectroscopy of graphene and graphite: disorder, electron–phonon coupling, doping and nonadiabatic effects, Solid State Commun. 143 (2007) 47–57, https://doi.org/10.1016/j.ssc.2007.03.052.

[275] V.A. Sethuraman, L.J. Hardwick, V. Srinivasan, R. Kostecki, Surface structural disordering in graphite upon lithium intercalation/deintercalation, J. Power Sources 195 (2010) 3655–3660, https://doi.org/10.1016/j.jpowsour.2009.12.034.

[276] J.R. Dahn, T. Zheng, Y. Liu, J.S. Xue, Mechanisms for lithium insertion in carbonaceous materials, Science 270 (1995) 590–593, https://doi.org/10.1126/science.270.5236.590, 80.

[277] A. Heckmann, J. Thienenkamp, K. Beltrop, M. Winter, G. Brunklaus, T. Placke, Towards high-performance dual-graphite batteries using highly concentrated organic electrolytes, Electrochim. Acta 260 (2018) 514–525, https://doi.org/10.1016/j.electacta.2017.12.099.

[278] K.V. Kravchyk, P. Bhauriyal, L. Piveteau, C.P. Guntlin, B. Pathak, M.V. Kovalenko, High-energy-density dual-ion battery for stationary storage of electricity using concentrated potassium fluorosulfonylimide, Nat. Commun. 9 (2018) 4469, https://doi.org/10.1038/s41467-018-06923-6.

[279] M. Winter, J.O. Besenhard, M.E. Spahr, P. Novák, Insertion electrode materials for rechargeable lithium batteries, Adv. Mater. 10 (1998) 725–763, https://doi.org/10.1002/(SICI)1521-4095 (199807)10:10<725::AID-ADMA725>3.0.CO;2-Z.

[280] K.V. Kravchyk, M.V. Kovalenko, Rechargeable dual-ion batteries with graphite as a cathode: key challenges and opportunities, Adv. Energy Mater. 9 (2019) 1901749, https://doi.org/10.1002/aenm.201901749.

[281] M. Mao, T. Gao, S. Hou, C. Wang, A critical review of cathodes for rechargeable Mg batteries, Chem. Soc. Rev. 47 (2018) 8804–8841, https://doi.org/10.1039/c8cs00319j.

[282] J. Bitenc, K. Pirnat, T. Bančič, M. Gaberšček, B. Genorio, A. Randon-Vitanova, R. Dominko, Anthraquinone-based polymer as cathode in rechargeable magnesium batteries, ChemSusChem 8 (2015) 4128–4132, https://doi.org/10.1002/cssc.201500910.

[283] J. Bitenc, K. Pirnat, G. Mali, B. Novosel, A. Randon Vitanova, R. Dominko, Poly (hydroquinoyl-benzoquinonyl sulfide) as an active material in Mg and Li organic batteries, Electrochem. Commun. 69 (2016) 1–5, https://doi.org/10.1016/j.elecom.2016.05.009.

[284] Z. Song, H. Zhou, Towards sustainable and versatile energy storage devices: an overview of organic electrode materials, Energy Environ. Sci. 6 (2013) 2280, https://doi.org/10.1039/c3ee40709h.

[285] N.S. Hudak, Chloroaluminate-Doped conducting polymers as positive electrodes in rechargeable aluminum batteries, J. Phys. Chem. C 118 (2014) 5203–5215, https://doi.org/10.1021/jp500593d.

[286] G. Mamantov, R. Marassi, US Patent 4 (63) (1977), 005.

[287] K. Tanemoto, R. Marassi, C.B. Mamantov, Y. Ogata, M. Matsunaga, J.P. Wiaux, G. Mamantov, Oxidation of sulfur in chloroaluminate melts of intermediate pCl, J. Electrochem. Soc. 129 (1982) 2237–2242, https://doi.org/10.1149/1.2123482.

[288] R. Marassi, Electrochemical and spectroscopic studies of sulfur in aluminum chloride-N-(n-Butyl)Pyridinium chloride, J. Electrochem. Soc. 132 (1985) 1639, https://doi.org/10.1149/1.2114180.

[289] U.T.W.G. (TWG), Integrated SET-Plan Action 7, (n.d).

[290] https://www.alcoa.com/global/en/what-we-do/elysis/default.asp, 2020.

[291] A. Perez, V. Quintero, H. Rozas, F. Jaramillo, R. Moreno, M. Orchard, Modelling the degradation process of lithium-ion batteries when operating at erratic state-of-charge swing ranges, in: 2017 4th Int. Conf. Control. Decis. Inf. Technol, IEEE, 2017, pp. 860–865, https://doi.org/10.1109/CoDIT.2017.8102703.

[292] T. Broux, F. Fauth, N. Hall, Y. Chatillon, M. Bianchini, T. Bamine, J. Leriche, E. Suard, D. Carlier, Y. Reynier, L. Simonin, C. Masquelier, L. Croguennec, High rate performance for carbon-coated Na 3 V 2 (PO 4) 2 F 3 in Na-ion batteries, Small Methods 3 (2019) 1800215, https://doi.org/10.1002/smtd.201800215.

[293] (n.d. http://www.tiamat-energy.com/ http://www.tiamat-energy.com/.